Check for updates

Received: 18 April 2019 | Revised: 14 February 2020 | Accepted: 18 February 2020

DOI: 10.1111/bph.15049

RESEARCH PAPER

Improved efficacy, tolerance, safety, and abuse liability profile of the combination of CR4056 and morphine over morphine alone in rodent models

Emanuele Sala[1,2] | Flora Ferrari[1] | Marco Lanza[1] | Chiara Milia[3] | Chiara Sabatini[1,2] | Albino Bonazzi[1] | Eleonora Comi[1] | Miriam Borsi Franchini[1] | Gianfranco Caselli[1] | Lucio Claudio Rovati[1]

[1]Rottapharm Biotech, Monza, Italy

[2]PhD program in Neuroscience, University of Milano-Bicocca, Monza, Italy

[3]School of Medicine and Surgery, University of Milano - Bicocca, Monza, Italy

Correspondence
Marco Lanza, Rottapharm Biotech, Via Valosa di Sopra 9, 20900 Monza MB, Italy.
Email: marco.lanza@rottapharmbiotech.com

Background and Purpose: Prolonged use of opioids causes analgesic tolerance and adverse effects including constipation and dependence. Compounds targeting imidazoline I_2 receptors are known to potentiate opioid analgesia in rodents. We investigated whether combination with the I_2 receptor ligand CR4056 could improve efficacy and safety of morphine and explored the mechanisms of the CR4056–opioid interaction.

Experimental Approach: We used the complete Freund's adjuvant (CFA) model in rats to study the effects of treatments on hyperalgesia, morphine tolerance and microglia activation as measured by immunofluorescence. Opioid-induced adverse effects were assessed in rodent models of morphine-induced constipation, sedation (open field, sedation rating scale, and rotarod), physical dependence (naloxone-induced withdrawal), and abuse (conditioned place preference-associated reward). Chemiluminescence assays tested CR4056 as allosteric modulator of μ-opioid receptors.

Key Results: CR4056 (ED_{50} = 4.88 mg·kg^{-1}) and morphine (ED_{50} = 2.07 mg·kg^{-1}) synergized in reducing CFA-induced hyperalgesia (ED_{50} = 0.52 mg·kg^{-1}; 1:1 combination). Consistently, low doses of CR4056 (1 mg·kg^{-1}) spared one third of the cumulative morphine dose administered during 4 days and prevented/reversed the development of tolerance to morphine anti-hyperalgesia. These opioid-sparing effects were associated with decreased activation of microglia, independent of CR4056 interactions on μ-opioid receptors. Importantly, the low doses of CR4056 and morphine that synergize in analgesia did not induce constipation, sedation, physical dependence, or place preference.

Abbreviations: 2-BFI, 2-(2-benzofuranyl)-2-imidazoline; 95% CL, 95% confidence limits; b.i.d., twice daily; CFA, complete Freund's adjuvant; CR4056, [2-phenyl-6-(1*H*-imidazol-1yl)]quinazoline; HPMC, hydroxypropylmethyl cellulose; I.I., interaction index; Iba1, ionized calcium-binding adapter molecule 1; MPE, percentage of the maximum possible effect; NAQ, 17-cyclopropylmethyl-3,14β-dihydroxy-4,5α-epoxy-6α-[(3′-isoquinolyl)acetamido] morphine; RM, repeated measures.

This is an open access article under the terms of the Creative Commons Attribution-NonCommercial-NoDerivs License, which permits use and distribution in any medium, provided the original work is properly cited, the use is non-commercial and no modifications or adaptations are made.
© 2020 The Authors. British Journal of Clinical Pharmacology published by John Wiley & Sons Ltd on behalf of British Pharmacological Society

Conclusion and Implications: We showed selective synergism between CR4056 and morphine as analgesics. Their combination showed an improved safety and abuse liability profile over morphine alone. CR4056 could be developed as an opioid-sparing drug in multimodal analgesia.

1 | INTRODUCTION

Current pharmacotherapy of acute and chronic pain is dominated by well-established drug classes such as narcotic analgesics, nonsteroidal anti-inflammatory agents and antidepressants. Opioids are still the drugs of choice for many painful conditions. Despite their analgesic benefits, there are disadvantages of using these substances long-term. Tolerance, constipation, sedation, physical dependence, and addiction are adverse effects that make the discovery of novel analgesics extremely important (Benyamin et al., 2008; Trang et al., 2015).

Tolerance is a physical result of repeated use of a drug. Continuous treatment with a fixed amount of opioid results in the development of tolerance, so larger doses will be necessary to obtain the same analgesic effect (Christie, 2008; Williams, Christie, & Manzoni, 2001), with the risk of adverse events. Physical dependence can be defined as a change in physiological conditions after repeated drug intake. The body adapts to the presence of opioid (Williams et al., 2001), and treatment discontinuation triggers a withdrawal syndrome characterized by severe physical symptoms. Although the terms dependence and addiction are often used interchangeably, they are different (Volkow & McLellan, 2016). Addiction is a psychological type of dependence characterized by a tendency towards compulsive drug seeking (Nestler, 1997; Volkow & McLellan, 2016).

Opioid prescriptions have soared during the last decades, with increases in public health spending (Dieleman et al., 2016) and, regrettably, in opioid misuse, abuse and addiction (Manchikanti et al., 2017). This trend has caused an escalation of serious and fatal adverse events (Rudd, Seth, David, & Scholl, 2016). Different approaches are under analysis to mitigate the risks, including limiting the prescribed opioid to the lowest effective dose (Volkow & McLellan, 2016). Researchers have proposed multimodal treatment programmes, that is, combination therapies of opioids and other analgesics, as a way to attain this goal (Mercadante, 2014; Raffa, 2001).

Growing evidence suggests that compounds targeting imidazoline I_2 receptors can be a novel class of analgesics. These receptors are a group of proteins that are widely distributed in the CNS and that contain a domain recognized by so-called I_2 receptor ligands (Li, 2017). One of these proteins was identified as brain creatine kinase (Kimura et al., 2009). Because the nature and signalling pathways of I_2 receptors remain poorly understood, I_2 receptor ligands are identified as putative agonists (e.g., **CR4056**, 2-BFI) or antagonists (e.g., idazoxan) based on their functional fingerprint. There is robust evidence that I_2 receptors allosterically modulate the activity of enzymes involved in the monoaminergic descending pathways of pain control (Li, 2017), in line with the fact that noradrenergic mechanisms contribute to their anti-hyperalgesic effects (Ferrari et al., 2011; Siemian, Wang, Zhang, & Li, 2018). Importantly, crosstalk between I_2 receptor ligands and the opioid system has been well documented in the locus coeruleus neurons (Ruiz-Durántez, Torrecilla, Pineda, & Ugedo, 2003). This interaction may favour opioid-sparing activity and be useful for the management of the adverse effects of opioids.

CR4056 is a reversible and selective I_2 receptor ligand with an IC_{50} value of 0.596 μM (Ki = 0.3 μM) in binding assays using rat brain membranes. CR4056 is endowed with potent anti-nociceptive and anti-hyperalgesic activity in different disease-based animal models (Comi et al., 2017; Ferrari et al., 2011; Lanza, Ferrari, Menghetti, Tremolada, & Caselli, 2014; Meregalli et al., 2012). Earlier studies showed that low doses of CR4056 and **morphine** had synergistic effects in rodent models of **capsaicin**-induced hyperalgesia (Ferrari et al., 2011)

What is already known

- CR4056 is a novel, potent analgesic acting as an imidazoline-2 receptor (I2R) ligand.
- Low doses of CR4056 and morphine synergize in analgesia in experimental animal models of pain.

What does this study add

- In rodents, the combination CR4056–morphine shows improved efficacy, safety, and abuse liability over morphine alone.
- First evidence linking attenuation of morphine tolerance by I_2 receptor ligands to decreased microglia activation/neuroinflammation.

What is the clinical significance

- Combinations of CR4056 and morphine could decrease opioid-induced tolerance, constipation, sedation, and abuse potential.
- These results support the clinical development of CR4056 as an opioid-sparing drug in multimodal analgesia.

14765381, 2020, 14, Downloaded from https://bpspubs.onlinelibrary.wiley.com/doi/10.1111/bph.15049 by University Studi Milano Bicocca, Wiley Online Library on [16/07/2024]. See the Terms and Conditions (https://onlinelibrary.wiley.com/terms-and-conditions) on Wiley Online Library for rules of use; OA articles are governed by the applicable Creative Commons License

and postoperative pain (Lanza et al., 2014). The objective of this work was to test the potential for use of CR4056 as an opioid-sparing drug in multimodal analgesia. We evaluated whether CR4056 could act synergistically with morphine in a combined regimen with improved tolerance, physical dependence, and abuse potential liabilities, and at doses that mitigated the adverse effects of opioids.

2 | METHODS

2.1 | Animals

All animal care and experimental procedures complied with national and international laws and policies on the protection of animals used for scientific purposes (Italian Legislative Decree 26/2014 that transposed the EU Directive 2010/63/EU; Guide for the Care and Use of Laboratory Animals, U.S. National Research Council, 2011), were approved by the Rottapharm Biotech Review Board, and were authorized by the Italian Ministry of Health (Decr. Min. #884/2015-PR, #60/2009-B, #214/2013-B, and #561/2017-PR). Animal studies are reported in compliance with the ARRIVE guidelines (Kilkenny, Browne, Cuthill, Emerson, & Altman, 2010; McGrath, Drummond, McLachlan, Kilkenny, & Wainwright, 2010) and with the recommendations made by the *British Journal of Pharmacology*.

Male Wistar rats (Charles River, Calco, Italy) weighing 250–300 g were housed with ad libitum access to food and water, in a temperature-controlled room with a 12-h light/dark cycle, at least 1 week before the beginning of the experiment. All studies in vivo except the conditioned place preference test were carried out during the light phase of the cycle. The total number of rats used was 844. At the end of experiments, rats were killed with CO_2 or by transcardial perfusion.

2.2 | Experimental design and drug treatments

Animals were assigned to experimental groups using a completely randomized design. Baseline measurements of mechanical hyperalgesia were comparable across groups after randomization. Experiments were designed to have equal groups of at least n = 5 and were performed by operators blind to treatments.

Morphine was dissolved in physiological saline and administered s.c.; naloxone was dissolved in physiological saline and administered i.p.; CR4056 was suspended in 0.5% hydroxypropylmethyl cellulose (HPMC) and administered orally. The oral route was chosen because CR4056 has good oral availability and is formulated for oral administration in humans (Rovati et al., 2020). Volumes of administration were 5 ml·kg^{-1} for CR4056 and naloxone and 2 ml·kg^{-1} for morphine. Naive, sham, and control animals always received the appropriate vehicles. The technical features of the experimental models used imposed different time intervals between CR4056 and morphine administration. The technical time required for oral gavage administration of CR4056 to different experimental groups was tested and set to a minimum of 15 min. Time of administration of each drug in each model is described in the relevant section.

Throughout this article, the term "sub-effective (or low) dose" refers to a dose of morphine or CR4056 that has no or marginal anti-nociceptive/anti-hyperalgesic efficacy per se (i.e., not in combination) in the CFA model of pain in rats.

2.3 | CFA model of chronic inflammatory pain

A total of 216 male Wistar rats were used in this model. Unilateral inflammation was induced 24 h before test drug administration by injecting 100 μl CFA (1 mg·ml^{-1} diluted 1:1 with saline; Sigma Aldrich) into the plantar surface of the right hind paw (Ferrari et al., 2011). Paw withdrawal threshold (i.e., the nociceptive threshold) to mechanical pressure was determined by Randall–Selitto test (Analgesy-Meter, Ugo Basile, Comerio, Italy).

2.3.1 | Acute effects

Following a single administration to rats, the peak plasma concentrations of morphine were recorded at ~10 min, whereas the peak plasma concentrations of CR4056 (in the range of pharmacological doses, 1–20 mg·kg^{-1}) occurred between 15 and 60 min. Consistently, studies in the CFA model in rats showed that the maximum anti-hyperalgesic activity of morphine and CR4056 was observed at about 30 and 90 min, respectively, after drug administration. Therefore, the acute effects of CR4056 and morphine, alone or in combination at different dosages, were evaluated (n = 6 per group) by administering CR4056 60 min before morphine in order to synchronize their peak effects.

2.3.2 | Opioid-sparing paradigm

Sub-effective doses of morphine and CR4056 were combined using a dosing schedule specifically designed to test morphine-sparing activity. In this novel paradigm, our aim was to mirror patient-controlled analgesia by maintaining anti-hyperalgesic efficacy constantly above a clinically relevant threshold (i.e., 50%). Briefly, 24 h after CFA injection, rats were randomly divided into two groups (n = 15 per group). One group was treated orally with vehicle, while the other was treated orally with 1 mg·kg^{-1} CR4056. A starting dose of 1 mg·kg^{-1} morphine s.c. was administered with a technical lag of 15 min because of the different administration routes, and Randall–Selitto test was performed 30 min after morphine administration. If the withdrawal threshold was equal or above 50% of efficacy, the subsequent morphine dose (8 h apart from the first one) did not change. If the experimental withdrawal threshold was below 50% of efficacy, morphine dose was increased by 1 mg·kg^{-1}. The efficacy of treatment was calculated by considering 100% the withdrawal threshold value

14765381, 2020, 14, Downloaded from https://bpspubs.onlinelibrary.wiley.com/doi/10.1111/bph.15049 by University Studi Milano Bicocca, Wiley Online Library on [16/07/2024]. See the Terms and Conditions (https://onlinelibrary.wiley.com/terms-and-conditions) on Wiley Online Library for rules of use; OA articles are governed by the applicable Creative Commons License

registered before CFA challenge and 0% the value registered before the first treatment. Each rat was considered as a unit, and morphine treatment was scaled based on its daily individual performance. This regimen was repeated twice daily (b.i.d.) for 4 days. Mechanical hyperalgesia was measured once a day, 30 min after the first daily morphine administration.

2.3.3 | Tolerance to morphine anti-hyperalgesia

A full analgesic dose of morphine (5 mg·kg^{-1}, s.c.) was administered sub-acutely (4 to 14 days of treatment; n = 6 per group). The oral dosing of CR4056 or its vehicle was scheduled with a technical lag of 15 min before the administration of morphine or saline. In a preventive paradigm of morphine tolerance, CR4056 (range 0.1–1 mg·kg^{-1}, p.o.) was administered starting from the beginning of morphine treatment. This regimen was repeated b.i.d. for 4 days. Mechanical hyperalgesia was measured on Days 1 and 4. In rescue (or reversal) experiments, tolerance was first induced by b.i.d. administration of morphine for 7 days, and then the treatment continued until Day 14 along with oral administration of 1 mg·kg^{-1} CR4056. The nociceptive threshold was measured on Days 1, 7, and 14.

2.4 | Spinal cord immunofluorescence assay

To evaluate the acute effects of an anti-hyperalgesic dose of CR4056 on microglia, 18 rats were divided into two groups: Six rats were used as a control group, while 12 rats were treated with intraplantar CFA. Three days after CFA challenge, rats were divided into two groups (vehicle and 6 mg·kg^{-1} CR4056; n = 6), tested for hyperalgesia (90 min after the oral treatment), and perfused as described below.

Instead, to study the microglial response of morphine-tolerant rats treated with a sub-effective dose of CR4056, 25 of the 216 rats used in the CFA model of inflammatory pain (see above; n = 5 per group) were deeply anaesthetized with an overdose of urethane (1.5 g·kg^{-1}, i.p.) 14 days after CFA injection. Rats were then transcardially perfused with 250 ml of 0.9% saline containing 1% heparin (5,000 UI·ml^{-1}), followed by 500 ml of 10% formalin (i.e., 4% paraformaldehyde, Bio-Optica Spa, Milan, Italy). The L5 segment of the spinal cord was harvested, post-fixed overnight at 4°C, and embedded in paraffin blocks for sectioning. Transverse sections of the spinal cord were sliced with a fully automated rotary microtome at 5-μm thickness, mounted on poly-L-lysine coated slides, and processed for immunofluorescence. Antigen retrieval was performed using 10-mM citrate buffer (pH 6.0) for 20 min at 90°C. The sections were blocked with 10% normal horse serum in PBS containing 0.3% Triton-X for 90 min at room temperature and then incubated overnight at 4°C with rabbit anti-ionized calcium-binding adapter molecule 1 (Iba1) primary polyclonal antibody (1:350; Wako Cat# 019–19,741, RRID:AB_839504). For secondary detection, sections were incubated for 1 h at room temperature with Alexa-Fluor 488 donkey anti-rabbit secondary antibody (1:400; ThermoFisher Scientific Cat #A-21206, RRID:AB_2535792). The slides were mounted with FluoroShield mounting medium with DAPI (Sigma Aldrich, #F6057) to counterstain the nuclei. Spinal cord sections were visualized with Invitrogen EVOS FL Auto Cell Imaging System (Thermo Fisher Scientific, Waltham, MA, USA). The contralateral side of each section was identified with a small cut in the ventral horn. Laminae I-III of the dorsal horns were identified taking as reference the rat brain atlas of Paxinos and Watson (1982). For each section, a representative image of both the ipsilateral and the contralateral dorsal horn (laminae I-III) of the L5 spinal cord was captured at 20× magnification, using consistent exposure times across all sections, and then analysed. Iba1-positive microglial cells displaying an amoeboid/activated state (i.e., clearly swollen cell bodies with reduced processes) were manually counted, as described previously (Sagar et al., 2011). Results are expressed as the percentage of the ipsilateral/contralateral ratio of the number of Iba1-positive microglial cells displaying an activated state. For each animal, six non-consecutive sections were analysed, and results were averaged.

2.5 | Cell-based assays

All chemiluminescence-based enzyme fragment complementation assays were performed by DiscoverX Corporation (Freemont, CA, USA), according to the manufacturer's instructions (http://www.discoverx.com).

β-arrestin 2 recruitment was assessed in transfected CHO-K1 cells (RRID:CVCL_KW43) using PathHunter® eXpress OPRM1 CHO-K1 β-Arrestin GPCR Assay (DiscoverX). Briefly, PathHunter eXpress β-Arrestin GPCR cells are engineered to co-express the GPCR (human μ-opioid receptor in this case) tagged to ProLink™ (PK, i.e., small fragment of β-galactosidase or β-gal) and β-arrestin 2 tagged to the Enzyme Acceptor (EA, i.e., large fragment of β-gal). When the EA-tagged β-arrestin 2 translocates to the PK-tagged μ-receptor due to μ-receptor activation, the complementary β-gal fragments interact to form a functional enzyme, which is detected by chemiluminescence. μ-opioid receptor internalization was evaluated in transfected U2OS cells (RRID:CVCL_LB02) using PathHunter™ Total GPCR Internalization Assay (DiscoverX), which works with the PK and EA fragment of β-gal fused to μ-opioid receptors and endosomes, respectively. μ-receptor activation leads to its internalization to endosomes, which generates a chemiluminescent signal following complementation of β-gal fragments. The decrease in cAMP intracellular levels after μ-opioid receptor activation, which is coupled to G_i protein, was assessed in transfected CHO-K1 cells by cAMP Hunter™ eXpress GPCR Assay (RRID:CVCL_KV62). Briefly, the enzyme donor (ED) fragment of β-gal is fused to cAMP and competes with intracellular cAMP for binding to a cAMP-specific antibody. A functional β-gal is formed by complementation of the exogenous EA to any unbound ED-tagged cAMP and produces a chemiluminescent signal directly proportional to the amount of intracellular cAMP (Burford et al., 2013). The μ-opioid receptors were activated by the

14765381, 2020, 14, Downloaded from https://bpspubs.onlinelibrary.wiley.com/doi/10.1111/bph.15049 by University Studi Milano Bicocca, Wiley Online Library on [16/07/2024]. See the Terms and Conditions (https://onlinelibrary.wiley.com/terms-and-conditions) on Wiley Online Library for rules of use; OA articles are governed by the applicable Creative Commons License

endogenous ligand [Met]-enkephalin at concentrations equal to its EC_{80} and EC_{20}, calculated in each assay, in order to investigate respectively a negative (NAM) and a positive (PAM) modulation. Data are expressed as percentage of efficacy using the formulae reported in the manufacturer's instructions. CR4056 was used at concentrations ranging from 0.1 to 10 μM.

2.6 | Morphine-induced constipation

The experiments were conducted according to the procedure described by Harada et al. (2017). Sixty-four Wistar rats (Charles River) were used in this model. Faecal excretion was evaluated at the end of the dark phase, when most activities and feeding of albino rats take place. Rats were housed two per cage, drugs were administered 2 h before the dark phase of the light/dark cycle, and the faeces were collected and counted 16 h after drug treatment. The number of faeces per cage was divided by two to obtain the number of faeces per rat, assuming a similar course of defecation between rats housed in the same cage. In this experimental paradigm, CR4056 was administered 15 min before morphine.

2.7 | Morphine-induced sedation

Opioid-induced sedation was examined using three experimental models in rats: the open field and rotarod for the evaluation of locomotor activity and coordination, the sedation rating scale for the description of signs and behaviours related to sedation. One hundred seventy-six Wistar rats (Charles River) were used for these experiments. The open field paradigm consisted of 4 days of treatment. Locomotor activity was recorded daily for 5 min. We chose a short duration of tracking so that habituation could be ruled out, and the control group maintained a constant level of exploration on repeated sessions. The experiments were performed according to the procedure described by Haleem and Nawaz (2017). Drugs were administered 60 min (CR4056 or its vehicle orally) and 30 min (morphine or its vehicle subcutaneously) before the open field test. The video tracking was performed using the software Ethovision XT 13 (RRID:SCR_000441; Noldus Information Technology).

Sedation rating scale consists of a panel of eight parameters (ocular ptosis, head position, posture, muscle tone, spontaneous movements, exploration, righting reflex, and corneal reflex) recorded by the operator after drug administration (Chuck, McLaughlin, Arizzi-LaFrance, Salamone, & Correa, 2006). Three sessions of observation were performed 15, 30, and 45 min after morphine administration. At each time point, a score from 0 (maximum sedation) to 5 (absent sedation) was assigned to each of the eight parameters. The sum of the scores produces the total score. Every observation was followed by rotarod for the evaluation of the impairment of motor coordination (Chuck et al., 2006). Rotarod paradigm had a duration of 2 days. On Day 1, every rat did four trials on the rotarod apparatus (Rota-Rod/RS, Panlab, Spain) at a constant speed of 5 r.p.m. during first and second trials and of 10 r.p.m. during third and fourth trials. For each trial, the time of endurance on rotarod (latency) was recorded, and the mean value was used to discard 20% of rats with the worse results. The cut-off during selection day was 2 min. The rats that passed the selection on Day 2 were randomly assigned to the experimental groups. The apparatus was set to acceleration mode. The speed of rotation increased from 0 to 40 r.p.m. in 5 min that is the cut-off of this phase of experiment. Four trials were performed during the test day: the first one immediately before treatment, the following trials 15, 30, and 45 min after treatment. Sedation includes a worsening of this type of performance.

2.8 | Morphine physical dependence and withdrawal

A method to quantify the degree of morphine physical dependence is to induce a withdrawal syndrome by administration of the opioid antagonist naloxone. Abrupt cessation of morphine effect by naloxone triggers a wide range of symptoms and behaviours in the animal. One hundred thirty-two Wistar rats (Charles River) were used in this model. They were randomly assigned to different experimental groups (n = 9/12) and were treated with morphine, CR4056, or their combination for 12 days, as previously described (Liu et al., 2018). Increasing doses and repeated fixed doses were tested in three different experiments. In the first one, rats were treated b.i.d. for 12 days with saline or increasing doses of morphine (s.c.) according to the following schedule: Day 1, 5 $mg{\cdot}kg^{-1}$; Day 2, 10 $mg{\cdot}kg^{-1}$; Day 3, 15 $mg{\cdot}kg^{-1}$; Day 4, 20 $mg{\cdot}kg^{-1}$; Day 5, 25 $mg{\cdot}kg^{-1}$; Day 6, 30 $mg{\cdot}kg^{-1}$; and Days 7–12, 35 $mg{\cdot}kg^{-1}$. Fixed doses of CR4056 (1 $mg{\cdot}kg^{-1}$, p.o., b.i.d. for 12 days) or its vehicle were administered 60 min before morphine. In the second paradigm, the schedule of morphine treatment was the same as that described above, while CR4056 was administered at increasing doses according to the following schedule: Day 1, 1 $mg{\cdot}kg^{-1}$; Day 2, 2 $mg{\cdot}kg^{-1}$; Day 3, 3 $mg{\cdot}kg^{-1}$; Day 4, 4 $mg{\cdot}kg^{-1}$; Day 5, 5 $mg{\cdot}kg^{-1}$; Day 6, 6 $mg{\cdot}kg^{-1}$; and Days 7–12, 7 $mg{\cdot}kg^{-1}$ (morphine–CR4056 ratio 5:1). The third study tested fixed doses of morphine and CR4056, both at 1 $mg{\cdot}kg^{-1}$, b.i.d.

On Day 12, 2 h after the morning morphine treatment, naloxone (5 $mg{\cdot}kg^{-1}$, i.p.) was administered to all rats. Animals were observed for 45 min to describe the severity of withdrawal symptoms (Liu et al., 2018). Jumping, writhing, wet dog shakes, yawning, head bobbing, and sweeping tail were recorded as frequency and then translated to scores (0 = none; 1 = 1–5 times; 2 = 6–10 times; and 3 = >10 times). For teeth chattering and chewing, the translation to scores was different (0 = none; 1 = 1–10 times; 2 = 11–20 times; and 3 = >20 times). Irritability, ocular ptosis, salivation, diarrhoea, altered breathing, lacrimation, and piloerection were recorded directly as scores (0 = none; 1 = mild; 2 = moderate; and 3 = severe). The sum of all scores was defined as global withdrawal score.

14765381, 2020, 14, Downloaded from https://bpspubs.onlinelibrary.wiley.com/doi/10.1111/bph.15049 by University Studi Milano Bicocca, Wiley Online Library on [16/07/2024]. See the Terms and Conditions (https://onlinelibrary.wiley.com/terms-and-conditions) on Wiley Online Library for rules of use; OA articles are governed by the applicable Creative Commons License

2.9 | Conditioned place preference

Conditioned place preference is a commonly used experimental paradigm that measures reward behaviours associated with abuse liability. This test exploits the tendency of rats to associate the environment where they are located with the effect of drugs administered during a conditioning period. The experiment was done in a wooden apparatus consisting of two lateral chambers (30 × 25 cm, length × width) with visual and tactile peculiarity and a central "neutral" chamber, smaller than the others (12 × 25 cm, length × width) with floor and walls total white. The lateral chambers had different decoration of walls (points or stripes) and different type of floor (smooth or rough). These differences were recognized by rats and associated with the effect of drug or vehicle treatment. All walls were 38.5 cm high.

Four days before the preconditioning phase, the light/dark cycle was inverted; all phases of experiments were performed in darkness. On the preconditioning day (Day 1), Wistar rats (Charles River) were placed in the neutral chamber, and for 15 min, they were free to explore all the environments of the apparatus, as described in the literature (van der Kam, De Vry, Schiene, & Tzschentke, 2008). The time spent in each chamber was recorded with a video tracking software (Ethovision XT 13, Noldus Information Technology). Rats that spent over 60% of time in one of two lateral chambers were not admitted to the conditioning phase. After preconditioning, rats were randomly assigned to the experimental groups (n = 16); 256 rats were used in this model. During the 2 days of conditioning phase, rats were treated with drug (Day 2) or vehicle (Day 3). On the first conditioning day, rats were treated with the active drug and were confined in the unpreferred lateral chamber during preconditioning (paired chamber), with no access to the other chambers of the apparatus for 40 min. On the second day of conditioning, rats were treated with vehicle and were located in the opposite chamber (unpaired chamber). A control group received vehicle in both chambers. CR4056 or its vehicle was administered 40 min before the conditioning, whereas morphine or its vehicle was administered immediately before the conditioning. There was no treatment on the test day (Day 4), where rats were placed in the neutral chamber with the possibility to explore all chambers of the apparatus. The time spent in each chamber was recorded. A significant difference between the mean time spent in paired versus unpaired chamber on the test day suggests the potential for a drug to induce preference (i.e., drug-seeking behaviour) (Mueller, Perdikaris, & Stewart, 2002).

2.10 | Data and statistical analysis

The data and statistical analysis comply with the recommendations of the *British Journal of Pharmacology* on experimental design and analysis in pharmacology (Curtis et al., 2015). Unless otherwise stated, results are reported as mean ± SEM. GraphPad Prism version 6.0 (RRID:SCR_002798; GraphPad Software Inc., San Diego, CA, USA) was used for statistical analysis. Significance was defined as $P < 0.05$. The graphs were made using SigmaPlot 13.0 (RRID:SCR_003210; Systat Software, San Jose, CA, USA).

In the experimental animal model of inflammatory pain, comparison between sham and CFA-treated rats was performed on mechanical threshold values (expressed in g) by Student's t test. The test was performed adjusting for heterogeneity of group variances. Crude mechanical threshold values (expressed in g) were also used for data analysis by one-way ANOVA in dose–response experiments. Post hoc comparisons were made using multiple comparison tests between experimental groups or within each experimental time.

In the experiments evaluating tolerance to morphine anti-hyperalgesia, data were analysed by repeated measures (RM) two-way ANOVA with treatment as the inter-subject variable and time as the intra-subject variable. No assumption of sphericity of the variance/covariance matrix was made; thus, the Geisser–Greenhouse correction was introduced. Post hoc comparisons were run using Dunnett's multiple comparisons test (i.e., multiple comparison against a control group) within each experimental time. Immunofluorescence data were analysed by one-way ANOVA followed by Tukey's multiple comparisons test.

In constipation experiments, data were expressed as number of faeces excreted from 5.00 PM to 9.00 AM. To evaluate statistical significance, data were analysed by Kruskal–Wallis test. Post hoc comparisons were run using Dunn's multiple comparisons test.

In studies of opioid-induced sedation, data were expressed as distance travelled in 5 min of video tracking for open field, as total score for sedation rating scale, and as time of latency for rotarod. To evaluate statistical significance, open field data were analysed by two-way ANOVA. Post hoc comparisons were run using Dunnett's multiple comparisons test. The statistical significance of sedation rating scale and rotarod results was analysed by one-way ANOVA and Tukey's multiple comparison test.

In the behavioural studies of physical dependence, the sum of the scores assigned to each sign of withdrawal represents the global withdrawal score. Statistical significance was evaluated by Kruskal–Wallis followed by Dunn's multiple comparison test.

In the experiments for the evaluation of conditioned place preference, the time spent in the two conditioning chambers was compared. Data were analysed by two-way ANOVA. Post hoc mean comparisons were made using Tukey's test.

2.11 | ED_{50} evaluation

The dose that produced 50% anti-hyperalgesic effect (ED_{50}) was calculated at the time corresponding to the peak effect, using a standard linear regression analysis of the log dose–response curve, assuming that 100% is the mean withdrawal threshold of sham rats treated with vehicle and 0% is the mean withdrawal threshold of CFA rats treated with vehicle. The regression analysis was performed on the single data points (six animals per dose on at least four doses) and not on the group means, taking into account also values higher than 100%

14765381, 2020, 14, Downloaded from https://bpspubs.onlinelibrary.wiley.com/doi/10.1111/bph.15049 by University Studi Milano Bicocca, Wiley Online Library on [16/07/2024]. See the Terms and Conditions (https://onlinelibrary.wiley.com/terms-and-conditions) on Wiley Online Library for rules of use; OA articles are governed by the applicable Creative Commons License

(i.e., reaching a hypoalgesic effect). The ED_{50} errors were calculated as 95% confidence limits or intervals (95% CL).

2.12 | Isobolographic analysis

The interaction of CR4056 with morphine was evaluated by administering fixed 1:1 weight ratio combinations of CR4056 and morphine (0.1 + 0.1 mg·kg^{-1}; 0.3 + 0.3 mg·kg^{-1}; 1 + 1 mg·kg^{-1}; 3 + 3 mg·kg^{-1}). Isobolographic analysis was performed as described by Tallarida, Porreca, and Cowan (1989). The isobologram was constructed by connecting the ED_{50} of CR4056 plotted on the ordinate with the ED_{50} of morphine plotted on the abscissa to obtain the additivity line. On this line, a theoretical additive ED_{50} (ED_{50} add) was calculated according to Miranda, Prieto, Puig, and Pinardi (2008) using the formula:

$$ED_{50\,add} = ED_{50\,CR4056}/(P_1 + R * P_2),$$

where R is the ratio between the ED_{50} of CR4056 alone to morphine alone, P1 is the proportion of CR4056, and P2 is the proportion of morphine in the total mixture.

The variance (Var) of ED_{50} add was calculated from the fraction (FR) of the ED_{50} in the combination as

$$Var\,ED_{50\,add} = Var\,ED_{50\,CR4056} * (FR_{CR4056})^2 + Var\,ED_{50\,morphine} * (FR_{morphine})^2.$$

From this variance(s), 95% CL of the theoretical additive ED_{50} were calculated.

To evaluate the statistical significance of the synergistic effect, the theoretical values calculated as described above were compared by a Student's *t* test to the ED_{50} values experimentally obtained for the drug combination. The interaction index (I.I.) was calculated as the ratio of the experimental ED_{50} to the theoretical ED_{50} (Miranda et al., 2008). Values lower than 1 are an indication of synergistic interactions.

2.13 | Materials

The chemicals used in these experiments were supplied as follows: the prototypical μ-opioid agonist morphine hydrochloride was supplied by S.A.L.A.R.S. (Como, Italy); the μ-opioid selective antagonist naloxone by Sigma Aldrich (Milan, Italy), and CR4056 ([2-phenyl-6-(1*H*-imidazol-1yl)]quinazoline; CAS Registry Number: 1004997-71-0) was synthesized by the Medicinal Chemistry Department of Rottapharm Biotech (Monza. Italy). The purity of the CR4056 batch used in all the experiments was 100% (w/w). The drug-related impurity content by HPLC was <0.05% (w/w).

2.14 | Nomenclature of targets and ligands

Key protein targets and ligands in this article are hyperlinked to corresponding entries in http://www.guidetopharmacology.org, the common portal for data from the IUPHAR/BPS Guide to PHARMACOLOGY (Harding et al., 2018) and are permanently archived in the Concise Guide to PHARMACOLOGY 2019/20 (Alexander, Christopoulos et al., 2019; Alexander, Fabbro et al., 2019).

3 | RESULTS

3.1 | Low doses of CR4056 and morphine synergize in the CFA model of chronic pain

Twenty-four hours after CFA, rats showed hyperalgesia to mechanical stimuli. The mean withdrawal threshold in CFA rats was significantly lower than that measured in sham rats (162.5 ± 4.6 g vs. 227.5 ± 7.2 g). The Δ threshold expressed in g between sham and CFA animals treated with vehicle was defined as 100% anti-hyperalgesic efficacy. Subcutaneous administration of morphine (1–10 mg·kg^{-1}) reversed CFA-induced hyperalgesia in a dose-dependent manner, with peak effect at 30 min and ED_{50} = 2.07 mg·kg^{-1} (95% CL = 1.54–2.77) (Figure 1a). In agreement with published data (Ferrari et al., 2011), also CR4056 (1–30 mg·kg^{-1}) significantly and dose-dependently reversed the established hyperalgesia, with peak effect at 90 min (ED_{50} = 4.88 mg·kg^{-1}; 95% CL = 3.13–7.62) (Figure 1b).

When CR4056 and morphine were combined in a fixed 1:1 weight ratio (CR4056 60 min before morphine to synchronize their peak effects), there was a clear decrease of the doses needed to reverse CFA-induced hyperalgesia (Figure 1c). Isobolographic analysis demonstrated a synergistic interaction (Figure 1d). The ED_{50} value for the combination CR4056–morphine (0.52 mg·kg^{-1}; 95% CL = 0.18–0.37) was much lower than that measured after administration of each drug alone (4.88 mg·kg^{-1} for CR4056; 2.07 mg·kg^{-1} for morphine). Moreover, the ED_{50} value predicted assuming an additive effect (2.91 mg·kg^{-1}; 95% CL = 1.00–2.10) was five times the ED_{50} of 0.52 mg·kg^{-1} obtained experimentally for the 1:1 combination of CR4056 and morphine. The interaction index (I.I.) was <0.2.

3.2 | CR4056 is an opioid-sparing drug

By using the CFA model, we set up a novel experimental paradigm based on a dosing schedule designed to test opioid-sparing activity (see Section 2). We compared morphine consumption in two groups of rats treated with 1 mg·kg^{-1} CR4056 or vehicle b.i.d. 15 min before morphine, which could be increased to keep the anti-hyperalgesic effect as constant as possible (i.e., ≥50%). As expected, acute treatment with 1 mg·kg^{-1} morphine + vehicle resulted in suboptimal control of hyperalgesia (19.9 ± 6.7% efficacy against a target ≥50%; Figure 2a). Rats treated with 1 mg·kg^{-1} morphine + CR4056, instead, reached the target efficacy (87.2 ± 7.2%) already after the first dose. Under the morphine administration rules described in Section 2, both groups then maintained the target efficacy throughout the study (Figure 2a; Figure S1 shows data of individual animals). Morphine consumption in rats co-administered with CR4056 was significantly less

14765381, 2020, 14, Downloaded from https://bpspubs.onlinelibrary.wiley.com/doi/10.1111/bph.15049 by University Studi Milano Bicocca, Wiley Online Library on [16/07/2024]. See the Terms and Conditions (https://onlinelibrary.wiley.com/terms-and-conditions) on Wiley Online Library for rules of use; OA articles are governed by the applicable Creative Commons License

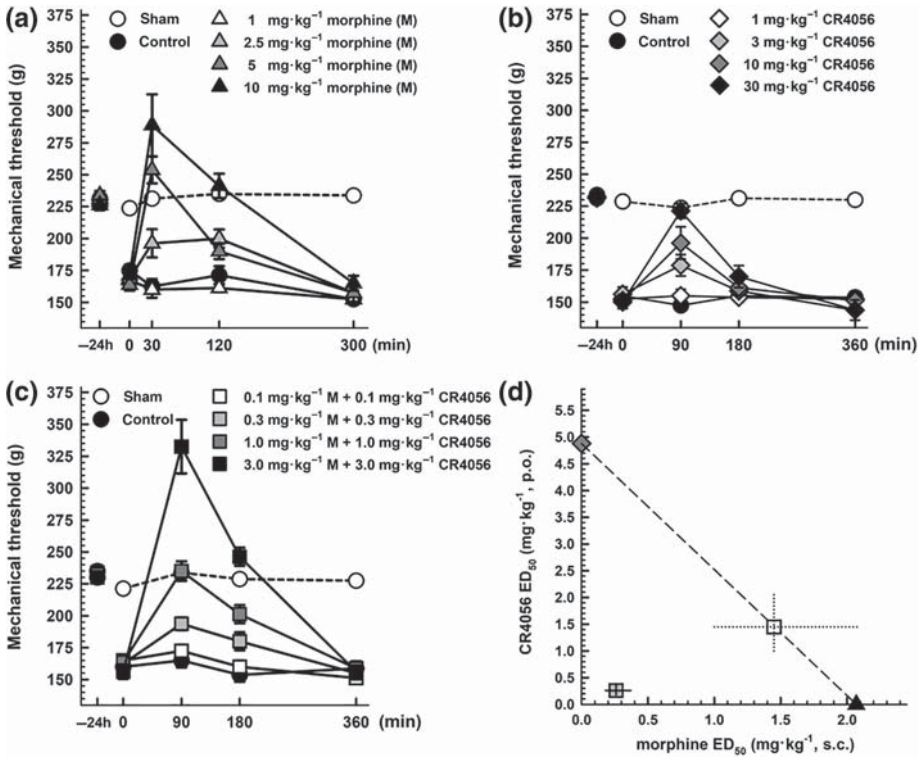

FIGURE 1 Synergistic effect of CR4056 and morphine. Anti-hyperalgesic effect of morphine and CR4056 either administered as single treatments (a, b) or co-administered in a 1:1 ratio (c). Morphine and CR4056 were acutely administered 24 h after CFA injection subcutaneously or orally, respectively. As morphine and CR4056 showed a different temporal response, we synchronized the peak effect of each drug by administering CR4056 1 h before morphine. Thus, mechanical hyperalgesia was measured 90, 180, and 360 min after CR4056 administration corresponding to 30, 120, and 300 min after morphine administration. Data shown are the means ± SEM (n = 6 per group) of the withdrawal threshold, expressed in grams. (d) Isobologram for the 1:1 combination of subcutaneous morphine with oral CR4056 in CFA-injected rats. The triangle corresponds to the experimental ED_{50} for morphine alone, the diamond represents the experimental ED_{50} for CR4056 alone, the grey square corresponds to the experimental ED_{50} for the 1:1 combination, and the open square corresponds to the ED_{50} value predicted assuming an additive effect. The time point upon the experimental data shown here were obtained 30 min after morphine administration

than in rats treated with vehicle. CR4056 spared 32.3 ± 7.5% morphine (Figure 2b). Even more importantly, only 2/15 (13%) of rats treated with morphine alone achieved the target efficacy maintaining the initial dose schedule (1 mg·kg^{-1}, b.i.d.), that is, consuming a total of 7 mg·kg^{-1} over 4 days. Conversely, the majority of rats (10/15, 67%) co-administered with 1 mg·kg^{-1} of CR4056, remained on the initial dose schedule of morphine (Figure S1).

3.3 | CR4056 prevents and reverses tolerance to morphine anti-hyperalgesic effects

Next, we investigated the modulation of morphine tolerance in the CFA model by co-administering sub-effective doses of CR4056 (0.1–-1 mg·kg^{-1}) with a full analgesic dose of morphine (5 mg·kg^{-1}). Drugs were given 15 min apart because of the different route, and this regimen was repeated b.i.d. for different time periods.

In a preventive paradigm, CR4056 and morphine were administered for a maximum of 4 days. On Day 1, CR4056 had no effects on morphine-induced anti-hyperalgesia (Figure 3a). On Day 4, anti-hyperalgesic efficacy decreased markedly in rats treated with repeated doses of morphine alone. The peak effect recorded 30 min after morphine was 150.8 ± 14.5% on Day 1 and 6.3 ± 8.3% on Day 4. CR4056 in the range 0.1–1 mg·kg^{-1} dose-dependently prevented the development of morphine tolerance. Post hoc analysis showed significant efficacy already at the lowest dose of CR4056 (Figure 3a).

In a rescue paradigm where the compound was co-administered with morphine from Day 7, when animals were tolerant to the opioid, CR4056 at 1 mg·kg^{-1} was even able to reverse morphine tolerance. Reversal occurred progressively until it was nearly complete on Day 14 (Figure 3b). This result also means that the combination of 5 mg·kg^{-1} morphine and 1 mg·kg^{-1} CR4056 did not induce tolerance.

3.4 | CR4056 decreases CFA- and morphine-induced spinal microglia activation

Microglia activation and neuroinflammation are present in chronic pain and are further induced by opioids. To study the cellular events whereby CR4056 attenuated morphine tolerance in the CFA model, we exploited the fact that microglia activation is characterized by morphological changes of cells from a ramified/resting phenotype to

14765381, 2020, 14, Downloaded from https://bpspubs.onlinelibrary.wiley.com/doi/10.1111/bph.15049 by University Studi Milano Bicocca, Wiley Online Library on [16/07/2024]. See the Terms and Conditions (https://onlinelibrary.wiley.com/terms-and-conditions) on Wiley Online Library for rules of use; OA articles are governed by the applicable Creative Commons License

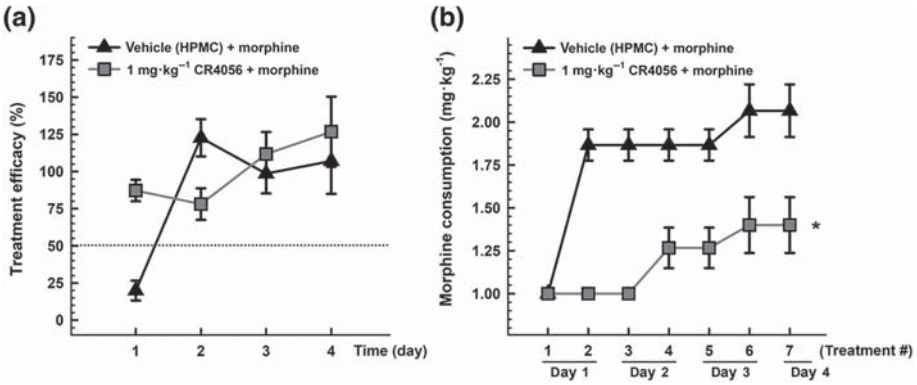

FIGURE 2 CR4056 as morphine-sparing drug. CR4056 or vehicle was administered orally to rats 15 min before morphine (4 days treatment; b.i.d.). Morphine starting dose was 1 mg·kg^{-1} (s.c.). Following morphine doses were titrated based on individual treatment efficacy determined by Randall–Selitto test. The efficacy of treatment was calculated by considering as 100% efficacy the individual withdrawal threshold measured before CFA injury and 0% efficacy the basal withdrawal threshold measured before the first morphine treatment. If the individual experimental threshold was equal or above 50% of efficacy, then the next morphine treatment remained the same as the previous morphine treatment. If the experimental withdrawal threshold was below 50% of efficacy, then the next morphine treatment increased by 1 mg·kg^{-1} relative to the previous morphine treatment. (a) Treatment efficacy in morphine-treated rats co-administered with 1 mg·kg^{-1} CR4056 or vehicle. Data represent mean values (% efficacy) ± SEM (n = 15 per group). (b) Morphine dose necessary to achieve the target efficacy (i.e., at least 50% of hyperalgesia reversion). Data represent mean values (mg·kg^{-1}) ± SEM (n = 15 per group). *P < .05, significantly different from vehicle; Student's t test

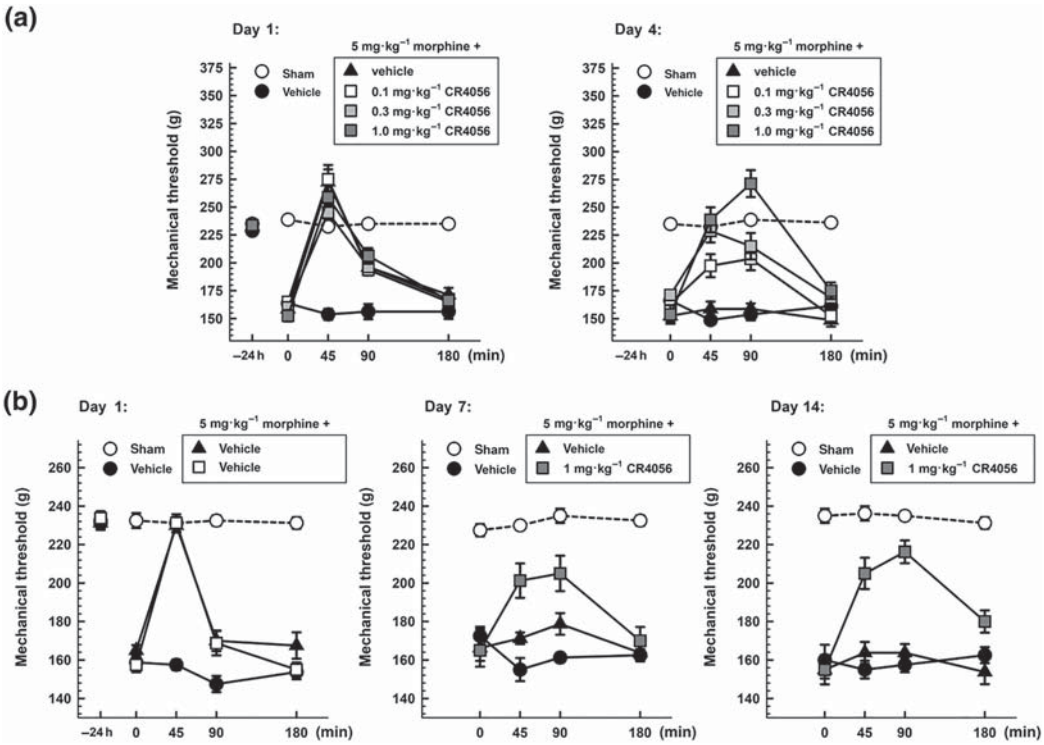

FIGURE 3 CR4056 prevents and reverses tolerance to morphine anti-hyperalgesia. (a) Effect of CR4056 on tolerance to morphine anti-hyperalgesia in the CFA model of chronic inflammatory pain in rats: preventive paradigm. A full analgesic dose of morphine (5 mg·kg^{-1}, s.c.) and CR4056 (range 0.1–1 mg·kg^{-1}, p.o.) was co-administered twice daily (b.i.d.) for 4 days. Mechanical threshold values (Randall–Selitto test) were assessed on Days 1 and 4 post-CFA. Data shown are the means ± SEM (n = 6 per group) of the withdrawal threshold, expressed in grams. (b) Effect of CR4056 on tolerance to morphine hyperalgesia in the CFA model of chronic inflammatory pain in rats: rescue paradigm. A full analgesic dose of morphine (5 mg·kg^{-1}, s.c.) was administered for 14 days (b.i.d.). CR4056 (1 mg·kg^{-1}, p.o.) was co-administered 15 min before morphine for 7 days (b.i.d.), starting 7 days after the beginning of morphine treatment. Mechanical withdrawal threshold values (Randall–Selitto test) were assessed on Days 1, 7, and 14 post-CFA. Data shown are the means ± SEM (n = 6 per group) of the withdrawal threshold, expressed in grams

14765381, 2020, 14, Downloaded from https://bpspubs.onlinelibrary.wiley.com/doi/10.1111/bph.15049 by University Studi Milano Bicocca, Wiley Online Library on [16/07/2024]. See the Terms and Conditions (https://onlinelibrary.wiley.com/terms-and-conditions) on Wiley Online Library for rules of use; OA articles are governed by the applicable Creative Commons License

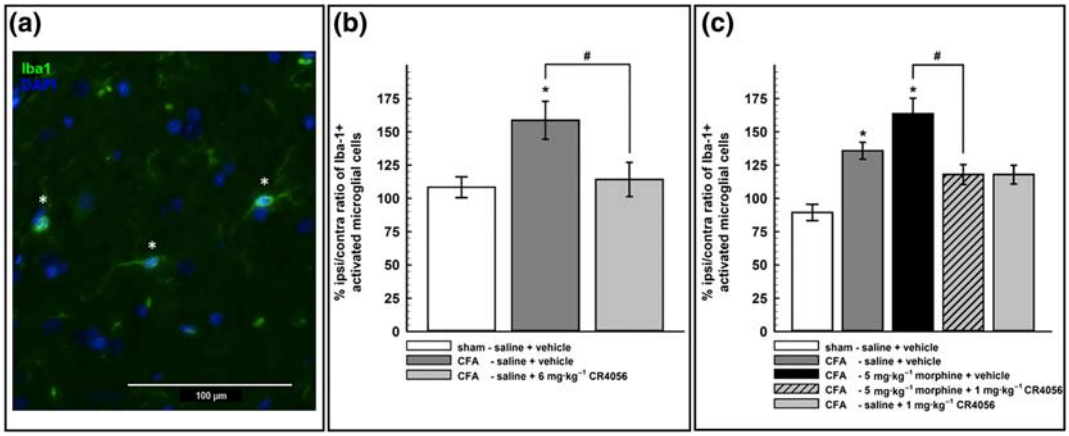

FIGURE 4 CR4056 decreases CFA- and morphine-induced spinal microglia activation. (a) Representative image of Iba1 and DAPI immunofluorescence staining in the ipsilateral dorsal horns (laminae I-III) of the L5 spinal cord, in CFA-injected rats. The quantification of microglia activation was determined as the number of Iba-1-positive microglia (i.e., indicated by asterisks), displaying a clearly swollen cell body with reduced processes. (b) Quantification of Iba-1 expression in the dorsal horn of L5 spinal cord 72 h after an intraplantar injection of saline (sham) or CFA, in rats acutely treated with vehicle (HPMC 0.5%) or CR4056 (6 mg·kg^{-1}, p.o.). Data shown are the mean percentage of the ipsilateral/contralateral ratio of Iba1 positive microglial cells displaying an amoeboid/activated state ± SEM (n = 6; six sections per animal). $^{*}P < .05$, significantly different from sham-vehicle treated group; $^{\#}P < .05$, significantly different from CFA-vehicle treated group; one-way ANOVA followed by Tukey's multiple comparison test. (c) Effect of CR4056 (1 mg kg^{-1}, p.o.) on microglia activation 14 days after the beginning of vehicle/morphine treatment in CFA-injected rats. Data represent the mean percentage of the ipsilateral/contralateral ratio of Iba1 positive microglial cells displaying an amoeboid/activated state ± SEM (n = 5; six sections per animal). $^{*}P < .05$, significantly different from sham-vehicle treated group; $^{\#}P < .05$, significantly different from CFA morphine-treated group; one-way ANOVA followed by Tukey's multiple comparison test

an amoeboid/activated state and by up-regulation of cell-surface markers such as Iba1 (Figure 4a).

Figure 4b shows microglia activation 3 days after CFA challenge, expressed as percentage of the ipsilateral/contralateral ratio of Iba1-positive microglial cells displaying an activated state. Acute treatment with 6 mg·kg^{-1} of CR4056, a dose eliciting clear anti-hyperalgesic effects, reduced microglia activation in the spinal cord of CFA-injected rats down to the levels observed in sham animals.

Using a subgroup of morphine-tolerant animals from the experiment shown in Figure 2b, we tested whether the dose of 1 mg·kg^{-1} CR4056 that reversed morphine tolerance could also affect microglia activation induced by repeated opioid administration. CFA injection per se significantly increased microglia activation by 52% (Figure 4c). Fourteen days of morphine (5 mg·kg^{-1}, b.i.d.) elicited a further activation of microglia in CFA-injected animals, with an increment of 83%, relative to sham rats. The low dose of 1 mg·kg^{-1} CR4056 did not affect CFA-induced microglia activation but significantly decreased morphine-induced activation of spinal microglia.

3.5 | CR4056 is not a positive or negative allosteric modulator of μ-opioid receptors

In receptor binding assays, CR4056 does not interact orthosterically with μ-opioid or other **opioid receptor subtypes** (Ferrari et al., 2011). To gain more insight into the mechanisms whereby CR4056 changes the response to morphine, an exploratory study assessed if μ-receptor internalization or the related β-arrestin and cAMP signals could be allosterically modulated by this compound (range 0.1–10 μM). The μ-receptor antagonist naloxone hydrochloride was used at 10 μM for comparison. CR4056 up to 10 μM did not act as a negative or positive allosteric modulator of cAMP signal, β-arrestin 2 recruitment, or human μ-receptor internalization induced by the orthosteric and endogenous ligand [Met]-enkephalin (Table S1). Thus, CR4056 seems to be neither an orthosteric ligand nor a positive/negative allosteric modulator of μ-opioid receptors.

3.6 | The low doses of CR4056 and morphine that synergize in analgesia do not induce constipation

Because a major goal of multimodal analgesia is to reduce the adverse reactions to opioids, additional experiments examined this issue. The potential effects of CR4056 on opioid-induced constipation were evaluated by counting the number of faeces excreted during 16 h after treatment. Different doses of morphine (range 5–30 mg·kg^{-1}; data not shown) were tested to identify a dose inducing a moderate constipation that could be modulated by co-treatment with CR4056. We chose a morphine dose of 10 mg·kg^{-1}, which decreased by ~30% faecal excretion (Figure 5a). Under these experimental conditions, co-administration of a full anti-hyperalgesic dose of CR4056 did not worsen opioid-induced constipation; rather, there was a trend for improvement. Importantly, the low doses of CR4056 and morphine that act synergistically in analgesia did not induce constipation when co-administered (Figure 5b).

14765381, 2020, 14, Downloaded from https://bpspubs.onlinelibrary.wiley.com/doi/10.1111/bph.15049 by University Studi Milano Bicocca, Wiley Online Library on [16/07/2024]. See the Terms and Conditions (https://onlinelibrary.wiley.com/terms-and-conditions) on Wiley Online Library for rules of use; OA articles are governed by the applicable Creative Commons License

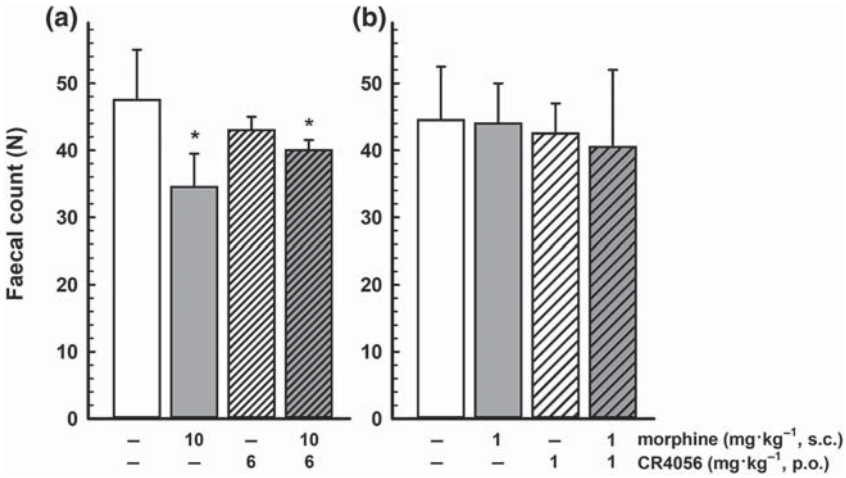

FIGURE 5 Effect of CR4056 on morphine-induced constipation. The number of faeces excreted was evaluated 16 h after drug treatment and is expressed as median with 95% confidence limit. (a) Morphine (10 mg·kg^{-1}, s.c.) decreased the number of faeces. *P < .05, significantly different from vehicle; Dunn's multiple comparisons test). The combination of morphine and CR4056 (6 mg·kg^{-1}) did not further reduce the number of faeces, compared with that after morphine alone. (b) Morphine and CR4056 co-administered at low doses (1 mg·kg^{-1}) did not decrease the number of faeces, compared with that after vehicle

3.7 | The low doses of CR4056 and morphine that synergize in analgesia do not induce sedation

Sedation is a typical adverse effect of opioids and can be measured by different methods. In this study, we used the open field, sedation rating scale, and rotarod paradigms. Monitoring of locomotor activity in the open field test showed a clear sedative effect of morphine at doses of 7.5 and 10 mg·kg^{-1}. Lower doses of morphine were not sedative, and in line with literature data in rodents (Nestler, 1997), there was a modest sensitization in the range 1–2.5 mg·kg^{-1}, as reflected by increased activity after 4 days of repeated treatment (Figure 6a). The low doses of morphine and CR4056 that act synergistically in analgesia did not induce sedation when co-administered (Figure 6b). In addition, CR4056 did not change the locomotor activity profile of non-sedative and sedative doses of morphine (2.5, 5, and 7.5 mg·kg^{-1}) (Figure 6c).

The performance of rats on sedation rating scale and rotarod worsened after acute treatment with increasing doses of morphine (range 1–20 mg·kg^{-1}; data not shown). A dose of 10 mg·kg^{-1} morphine (Figure 7a, b) was partially sedative in these models and was therefore used for the evaluation of potential synergistic interactions with CR4056. Low and high doses of CR4056 (1 and 6 mg·kg^{-1}, respectively) did not further worsen but tended to improve the performance of rats treated with 10 mg·kg^{-1} morphine, with a significant difference in sedation score at the higher dose of CR4056. There were no significant changes in performance versus control rats when morphine was administered at a dose of 1 mg·kg^{-1}, alone or in combination with CR4056 (Figure 7c, d).

3.8 | The low doses of CR4056 and morphine that synergize in analgesia do not induce physical dependence

Similar results were found in an experimental model of physical dependence where abrupt cessation of the opioid effect by naloxone triggers a withdrawal crisis with the appearance of signs and behaviours that can be measured in animals: diarrhoea, salivation, irritability, head bobbing, jumping, wet dog shakes, ocular ptosis, teeth chattering, and chewing. The sum of the scores associated with each behaviour defines the "global withdrawal score" (Liu et al., 2018).

After 12 days of treatment with escalating subcutaneous doses of morphine (up to 35 mg·kg^{-1}, b.i.d.), naloxone-induced withdrawal syndrome was marked and was not worsened by CR4056 co-administration (Figure 8a, b). Rather, there was a trend for improvement of global score when fixed or increasing doses of CR4056 were combined with increasing doses of morphine (Figure 8a, b).

No naloxone-induced crisis occurred instead when the low doses of CR4056 and morphine that synergize in analgesia were co-administered for 12 days in this experimental paradigm (Figure 8c).

3.9 | The low doses of CR4056 and morphine that synergize in analgesia do not induce place preference

To strengthen the pharmacological profiling of CR4056 in multimodal analgesia, we used conditioned place preference, a common experimental paradigm for exploring a drug's abuse potential in rodents. Conditioning with the test drugs was made in the preconditioning unpreferred chamber, which became the drug-paired chamber. There was no difference between groups in the time spent in paired and unpaired chambers during the preconditioning phase.

Doses of morphine ≥2.5 mg·kg^{-1} induced place preference, as reflected by a significant increase in the time that rats spent in paired chamber (Figure 9a), thus confirming the abuse potential of this drug. Figure 9b shows that no place preference occurred when animals received CR4056. Combined treatment with the low doses of CR4056 and morphine that synergize in analgesia did not induce place preference (Figure 9c). Finally, CR4056 did not potentiate the place preference induced by an addictive dose of morphine (Figure 9d).

4 | DISCUSSION

The concept behind multimodal analgesia is to mitigate the unwanted effects of opioids by facilitating their use at the lowest effective

14765381, 2020, 14, Downloaded from https://bpspubs.onlinelibrary.wiley.com/doi/10.1111/bph.15049 by University Studi Milano Bicocca, Wiley Online Library on [16/07/2024]. See the Terms and Conditions (https://onlinelibrary.wiley.com/terms-and-conditions) on Wiley Online Library for rules of use; OA articles are governed by the applicable Creative Commons License

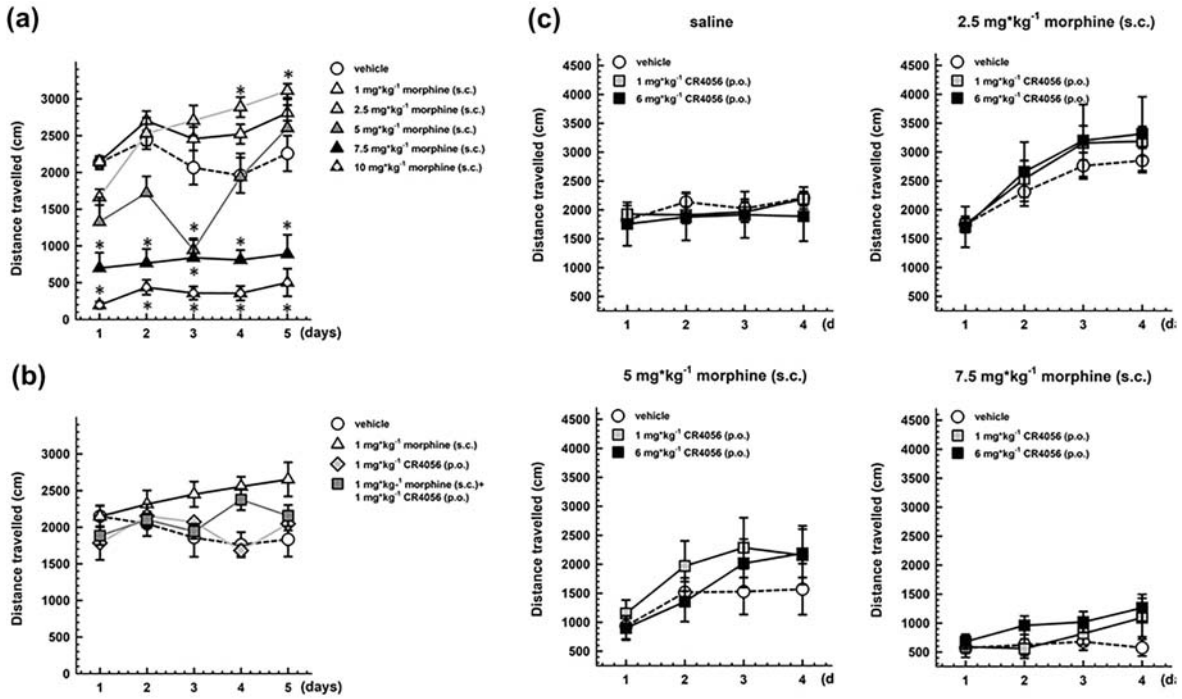

FIGURE 6 Effect of CR4056 on morphine-induced sedation: open field. (a) Effect of morphine administration on locomotor activity. Rats were treated s.c 30 min before the open field test every day for 5 days. Data shown are the distance (cm) travelled in 5 min (means ± SEM; $n = 6$ per group). $^*P < .05$, significantly different from vehicle; two-way ANOVA; Tukey's multiple comparison test. (b) Effect of morphine and CR4056 co-administration (1 mg·kg^{-1}) on locomotor activity. Rats were treated with morphine or saline s.c., 30 min before the open field test every day for 5 days. CR4056 was administered 30 min before morphine. Either given alone or in combination with morphine, CR4056 did not affect the locomotor activity. Data shown are the distance (cm) travelled in 5 min (means ± SEM; $n = 6$ per group); two-way ANOVA; Tukey's multiple comparison test. (c) Effect of CR4056 (1 and 6 mg·kg^{-1}, p.o.) on locomotor activity in the absence or presence of increasing doses of morphine (2.5, 5, and 7.5 mg·kg^{-1}). Rats were treated with morphine or saline s.c., 30 min before the open field test every day for 5 days. CR4056 was administered 30 min before morphine. Either given alone or in combination with morphine, CR4056 did not affect the locomotor activity. Data shown are the distance (cm) travelled in 5 min (means ± SEM; $n = 6$ per group); two-way ANOVA; Tukey's multiple comparison test)

doses. Potential benefits range from improved efficacy to decreased risks. In this study, the combination of low doses of CR4056 and morphine in animal models produced synergism in analgesia, absence of adverse reactions such as constipation and sedation, and no addictive properties (Table 1). CR4056 also attenuated morphine tolerance, an effect associated with a significant drop in opioid-induced microglia activation, a marker of neuroinflammation.

It is recognized that non-neuronal cells play a role in the development of tolerance to opioids (Hutchinson et al., 2011; Varrassi et al., 2018). Opioid-induced changes in microglial cells contribute to the hyperactivity of dorsal horn neurons, which could result in decreased analgesic efficacy (DeLeo, Tanga, & Tawfik, 2004; Hutchinson et al., 2011). Evidence exists that morphine tolerance can be attenuated in rodents by glial modulators (Horvath, Romero-Sandoval, & De Leo, 2010; Raghavendra, Tanga, & DeLeo, 2004) or inhibitors of spinal pro-inflammatory cytokines (Shen et al., 2011). Opioid-induced microglial responses can also occur via neuron–glia interactions (Varrassi et al., 2018). To investigate the cellular events whereby CR4056 prevented or reversed morphine tolerance in the CFA model, we examined the dorsal horns of lumbar spinal cord and found that CR4056 significantly decreased morphine-associated microglia activation, as measured by Iba1 staining. Attenuation of spinal neuroinflammation by an I_2 receptor ligand (2-BFI) was observed in a model of chronic pain by Siemian, LaMacchia, et al. (2018), but their findings did not involve opioid-induced changes. Because I_2 receptors are expressed in both neurons and glia (Keller & García-Sevilla, 2015), the effects of I_2 receptor ligands on neuroinflammation may be partially driven by a direct action on microglia and astrocytes (Siemian. LaMacchia, et al., 2018). Our results add to this stream of data. They associate the ability of the I_2 receptor ligand CR4056 to attenuate spinal microglia activation with the reversal of morphine tolerance.

To further study the mode of action of CR4056 in combination with morphine, we examined its relations with opioid signalling. CR4056 does not interact orthosterically with the μ or other opioid receptors (Ferrari et al., 2011), but there was still the possibility for the compound to be an allosteric modulator of this system. The μ-opioid subtypes are G_i/G_o protein-coupled receptors that upon agonist binding decrease cAMP synthesis, block Ca^{2+} influx, and reduce pain perception (Al-Hasani & Bruchas, 2011; Ninković & Roy, 2013). By contrast, prolonged opioid exposure leads to a compensatory increase of cAMP levels (Cahill, Walwyn, Taylor, Pradhan, & Evans, 2016; Ninković & Roy, 2013). Opioid tolerance is mainly mediated by desensitization, internalization, and down-regulation of

14765381, 2020, 14, Downloaded from https://bpspubs.onlinelibrary.wiley.com/doi/10.1111/bph.15049 by University Studi Milano Bicocca, Wiley Online Library on [16/07/2024]. See the Terms and Conditions (https://onlinelibrary.wiley.com/terms-and-conditions) on Wiley Online Library for rules of use; OA articles are governed by the applicable Creative Commons License

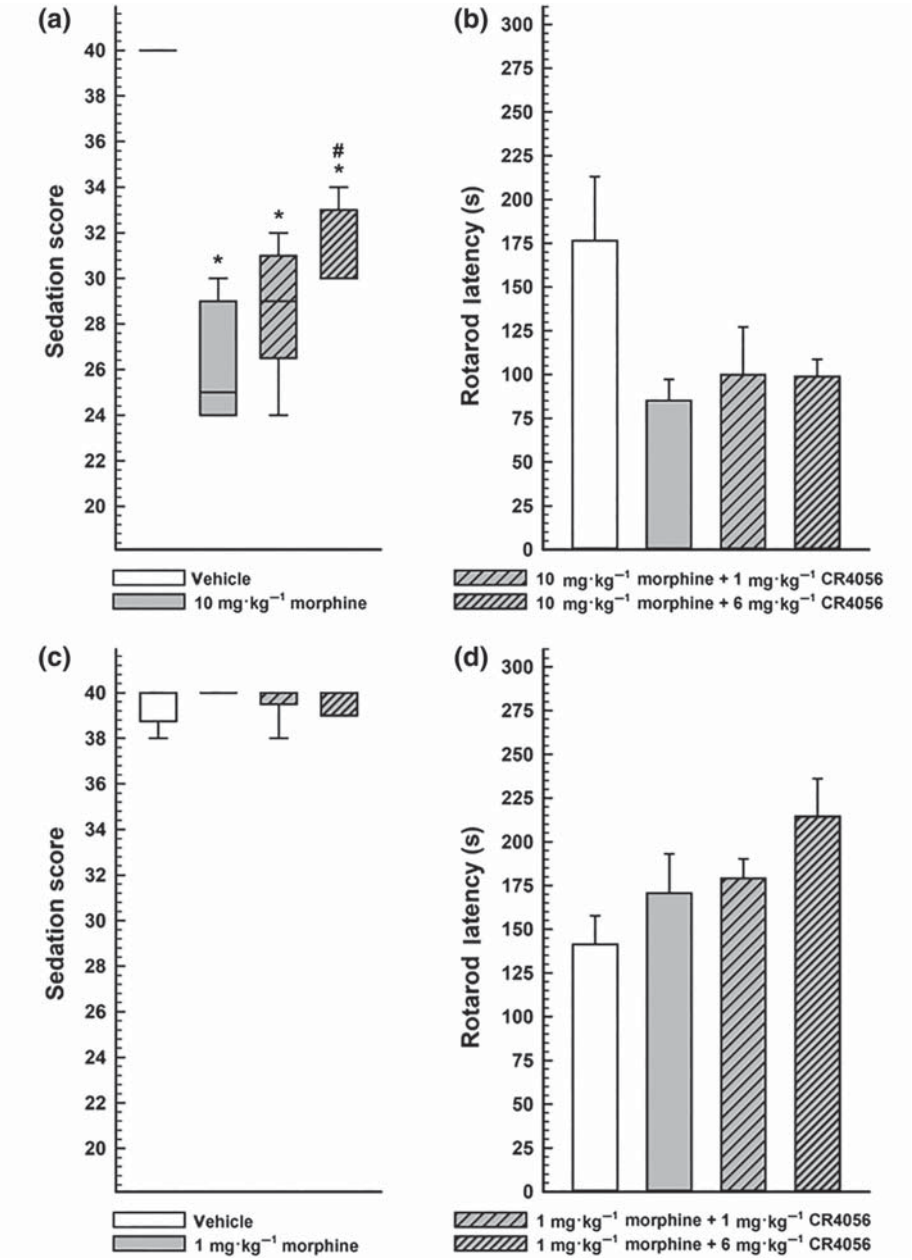

FIGURE 7 Effect of CR4056 on morphine-induced sedation: sedation rating scale and rotarod. Effect of CR4056 (1 and 6 mg·kg^{-1}, p.o.) on selected behaviours evaluated with the sedation rating scale (a, c) and motor coordination evaluated with rotarod (b, d) in the presence of a full analgesic (10 mg·kg^{-1}; a, b) or a sub-analgesic (1 mg·kg^{-1}; c, d) dose of morphine. Data represent sedation scores (a, c; box and whiskers plot where the box indicates the 25th and 75th percentiles, the whiskers indicate the 10th and 90th percentiles and the line within the box marks the median) and latency times (b, d; mean ± SEM expressed in s) registered 30 min after morphine administration. *P < .05, significantly different from vehicle; #P < .05, significantly different from 10 mg·kg^{-1} morphine-treated group; one-way ANOVA followed by Tukey's multiple comparison test

μ-opioid receptors (Al-Hasani & Bruchas, 2011). The β-arrestin pathway, which is triggered by μ-opioid receptor activation, is a key regulator of desensitization and internalization and thus promotes tolerance to opioids (Cahill et al., 2016; Kliewer et al., 2019). Indeed, knockout mice lacking β-arrestin 2 show enhanced analgesic responses to morphine with a concurrent attenuation of morphine-induced tolerance after repeated treatment (Bohn, Lefkowitz, & Caron, 2002). Our results here indicated that CR4056 is not an allosteric modulator of μ-opioid receptor internalization or β-arrestin 2 and cAMP signals. Further investigations are required to elucidate the molecular mechanisms whereby I_2 receptors interact with opioids in enhancing morphine analgesia and in decreasing tolerance to morphine. This missing element, despite our attempts, is the main limitation of the study.

In this respect, concurrent findings show that CR4056 inhibits PKCε translocation in rat sensory neurons (Vellani et al., 2020), a cellular event shared with other analgesics (Vellani & Giacomoni, 2017). As challenging as it has been thus far to identify a common mechanism for the many pharmacological properties of I_2 receptor ligands, PKCε translocation may be an important piece of the puzzle. The PKCε intracellular pathway is closely related to pain transmission through IB4$^+$ DRG neurons (Hucho, Dina, & Levine, 2005). Fast ATP-induced P2X currents are mediated by P2X3 receptors in IB4$^+$ DRG neurons (Petruska, Cooper, Johnson, & Gu, 2000). Consistent with these findings, a P2X3 antagonist was found to reverse tolerance to morphine antinociception (Ma, Xu, Xu, & Jiang, 2015) and to synergize with the endogenous opioid enkephalin in a model of cancer-induced hyperalgesia in mice (González-Rodríguez et al., 2017).

14765381, 2020, 14, Downloaded from https://bpspubs.onlinelibrary.wiley.com/doi/10.1111/bph.15049 by University Studi Milano Bicocca, Wiley Online Library on [16/07/2024]. See the Terms and Conditions (https://onlinelibrary.wiley.com/terms-and-conditions) on Wiley Online Library for rules of use; OA articles are governed by the applicable Creative Commons License

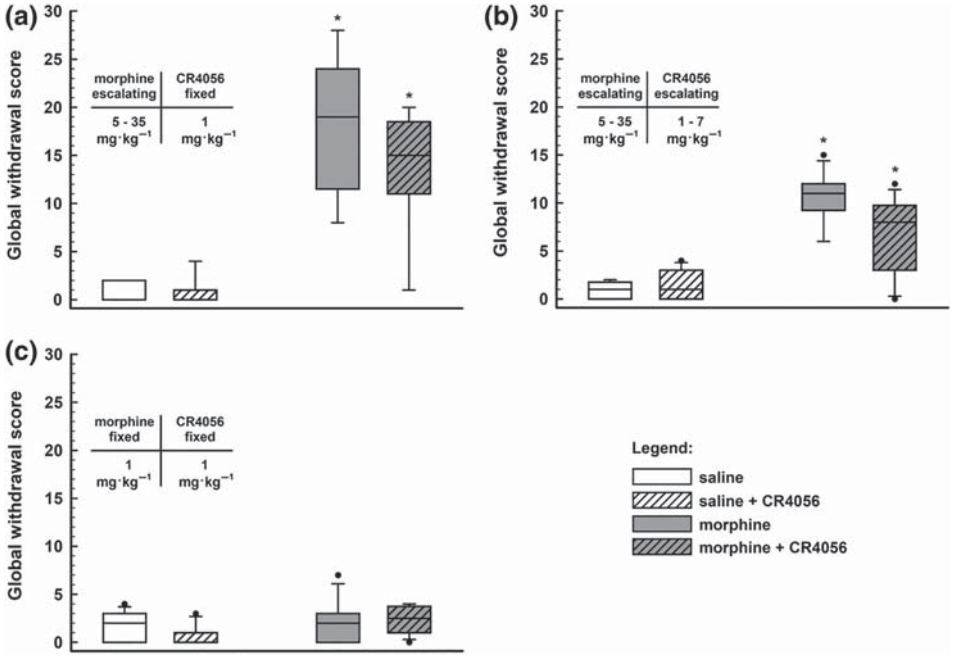

FIGURE 8 Effect of CR4056 on morphine-induced physical dependence. Global withdrawal scores in rats. Data are shown as a box and whiskers plot. The boundaries of the box indicate the 25th and 75th percentiles, while a line within the box marks the median. Whiskers indicate the 10th and 90th percentiles. Outlying points are marked below or above the whiskers. (a) Rats were treated with increasing doses of morphine from 5 to 35 mg·kg^{-1}, b.i.d. for 12 days (s.c.) and/or a fixed dose of 1 mg·kg^{-1} CR4056 (b.i.d.; p.o.). *P < .05, significantly different from saline; Kruskal–Wallis followed by Dunn's multiple comparison test; n = 9. (b) Rats were treated with increasing doses of morphine from 5 to 35 mg·kg^{-1}, b.i.d. for 12 days (s.c.) and/or with increasing doses of CR4056 from 1 to 7 mg·kg^{-1}, b.i.d. for 12 days (orally). *P < .05, significantly different from saline; Kruskal–Wallis followed by Dunn's multiple comparison test; n = 12. (c) Rats were treated with a fixed dose of 1 mg·kg^{-1} morphine (b.i.d.; s.c.) and/or a fixed dose of 1 mg·kg^{-1} CR4056 (b.i.d.; p.o.). There were no significant effects of the treatments; Kruskal–Wallis followed by Dunn's multiple comparison test; n = 12

The evidence of a synergism between CR4056 and morphine in analgesia is constant across different rodent models of pain (Ferrari et al., 2011; Lanza et al., 2014). A recent review (Li, 2017) reports examples of opioid-I_2 receptor ligand interactions being synergistic or additive depending on the efficacy of the opioid component on its receptor. In particular, 2-BFI shows synergistic interactions with lower efficacy opioids like **buprenorphine** but additive interactions with higher efficacy opioids like **fentanyl** (Siemian, Obeng, Zhang, Zhang, & Li, 2016). I_2 receptor ligands do not alter acute nociception but are effective for persistent and chronic pain. And because I_2 receptor ligands shift the opioid dose-effect curve leftward, their use has been envisaged in a multimodal pain therapy that reduces the opioid dose, which can be clinically significant (Li, 2017). In fact, CR4056 demonstrated opioid-sparing activity in a novel paradigm of repeated morphine administration in rats designed to mirror patient-controlled analgesia. Other drugs claimed to have opioid-sparing activity have been tested in non-clinical studies only for synergy after single administration. For instance, the α_2 adrenoceptor agonist **dexmedetomidine** was reported to be 4 times more potent when combined with morphine (Kabalak, Ekmekçioğlu, Ceylan, & Kahveci, 2013) and spared 20% morphine in a clinical trial for the treatment of postoperative pain (Li et al., 2018).

Another claimed potential for I_2 receptor ligands is to lessen opiate addiction (Bektas, Nemutlu, & Arslan, 2015; Sastre, Ventayol, & García-Sevilla, 1996). The addiction profile of morphine and other opioids is well described in the literature, but this adverse effect has been underestimated. Recent statistics by the National Institute on Drug Abuse (2019) show that every day more than 130 people in the United States die from opioid overdose. Abuse and addiction play a major role. The NIH has launched the HEAL (Helping to End Addiction Long-term) Initiative, an aggressive effort to speed solutions to stem the opioid public health crisis (including safe, effective, non-addictive strategies for chronic pain). The present study reproduced, in rodents, some behavioural features of morphine abuse potential. Remarkably, our experiments also show how these features were not present when the low doses of CR4056 and morphine that have synergistic anti-hyperalgesic effects were combined, suggesting reduced abuse potential.

Distinguishing the addiction profile of a drug from its potential to induce physical dependence is important. Little is known about the effects that I_2 receptor agonists have on the development of physical dependence, with few studies suggesting a role of I_2 receptor agonists in the modulation of opioid-induced dependence (Hudson et al., 1999; Thorn, Zhang, & Li, 2016). One method of quantifying the degree of physical dependence in animals is to use the opioid antagonist naloxone to induce a withdrawal syndrome. Our results in this paradigm outlined a safe profile for CR4056 and morphine co-administered at doses that act synergistically in analgesia.

14765381, 2020, 14, Downloaded from https://bpspubs.onlinelibrary.wiley.com/doi/10.1111/bph.15049 by University Studi Milano Bicocca, Wiley Online Library on [16/07/2024]. See the Terms and Conditions (https://onlinelibrary.wiley.com/terms-and-conditions) on Wiley Online Library for rules of use; OA articles are governed by the applicable Creative Commons License

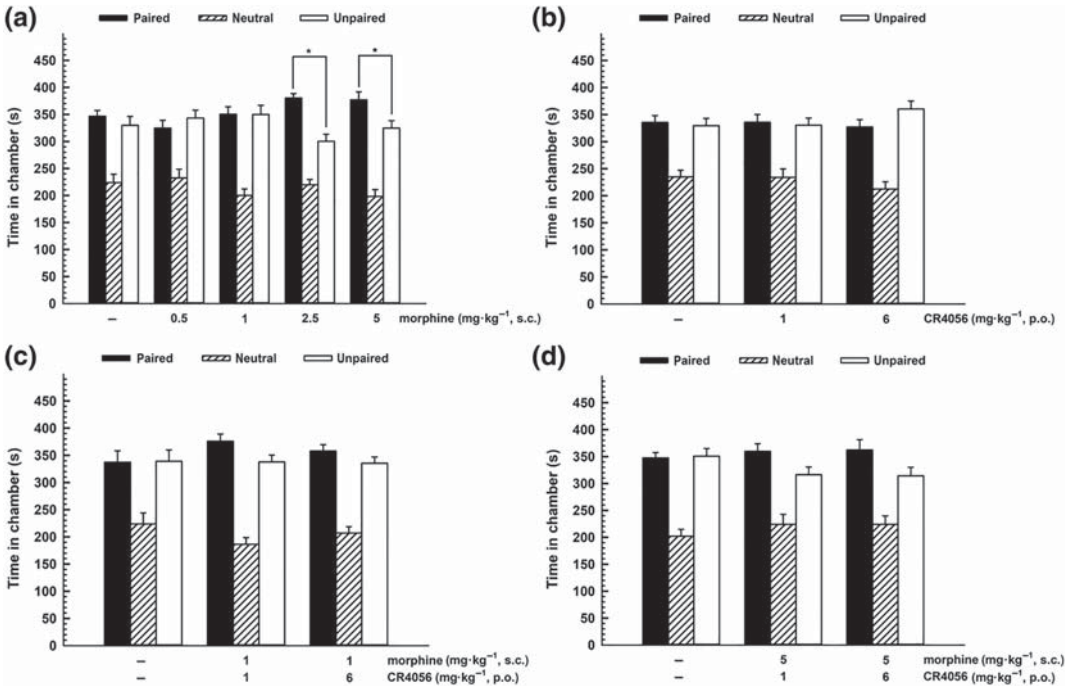

FIGURE 9 Effect of CR4056 on morphine-induced place preference. (a) Effect of morphine (range 0.5–5 mg·kg^{-1}; s.c.) on place preference. Mean (±SEM) of time spent in morphine-paired, neutral, and saline-paired chamber during 15′ on test day. *P < .05, significantly different from saline-paired side; two-way ANOVA followed by Tukey's multiple comparison test; n = 16 per group. (b) Effect of CR4056 (range 1–6 mg·kg^{-1}; p.o.) on place preference. Mean (±SEM; n = 16) of time spent in CR4056-paired, neutral, and saline-paired chamber during 15′ on test day. The effects of CR4056 were not different from those of the vehicle. Two-way ANOVA followed by Tukey's multiple comparison test. (c) Effect of co-administration of 1 mg·kg^{-1} morphine and CR4056 (range 1–6 mg·kg^{-1}; p.o.) on place preference. Mean (±SEM; n = 16) of time spent in drug-paired, neutral, and saline-paired chamber during 15′ on test day. CR4056, at either dose, did not modify the effects of morphine. Two-way ANOVA followed by Tukey's multiple comparison test. (d) Effect of co-administration of 5 mg·kg^{-1} morphine and CR4056 (range 1–6 mg·kg^{-1}; p.o.) on place preference. Mean (±SEM; n = 16) of time spent in drug-paired, neutral, and saline-paired chamber during 15′ on test day. CR4056, at either dose, did not modify the effects of morphine. Two-way ANOVA followed by Tukey's multiple comparison test (n = 16)

TABLE 1 Synoptic summary of reported results

	Antinociceptive effect compared with CFA-vehicle group	Microglia activation compared with CFA-vehicle group	Opioid adverse effects compared with vehicle group
CR4056 low dose	No	↔	No
CR4056 high dose	Yes	↓	No
Morphine low dose	No	n.d.	No
CR4056 low dose + morphine low dose	Yes	n.d.	No
Morphine high dose	Yes	↑	Tolerance Constipation, Sedation, Withdrawal
CR4056 low dose + Morphine high dose	Yes	↓ compared with morphine alone	↓ Tolerance ↔↓ Constipation, ↔↓ Sedation, ↔↓ Withdrawal

Note. CR4056: low dose = 1 mg·kg^{-1}; high dose ≥ 6 mg·kg^{-1}. Morphine: low dose = 1 mg·kg^{-1}; high dose ≥ 5 mg·kg^{-1}. n.d., not determined, ↓ reduced, ↔ unmodified.

To rule out the possibility that synergism also existed for the typical adverse reactions to opioids, CR4056 was studied in rodent models of morphine-induced constipation and sedation. Activation of μ-opioid receptors in the gastrointestinal tract inhibits propulsive peristalsis, thus slowing intestinal transit. Opioid-induced constipation is common and can arise at any time during treatment,

14765381, 2020, 14, Downloaded from https://bpspubs.onlinelibrary.wiley.com/doi/10.1111/bph.15049 by University Studi Milano Bicocca, Wiley Online Library on [16/07/2024]. See the Terms and Conditions (https://onlinelibrary.wiley.com/terms-and-conditions) on Wiley Online Library for rules of use; OA articles are governed by the applicable Creative Commons License

because tolerance develops to the analgesic effects and upper gastrointestinal motility but not in the colon (Akbarali, Inkisar, & Dewey, 2014). A multinational survey of patients receiving opioid therapy for chronic pain found that a third of them, despite the use of laxatives, had to reduce or stop using their opioid dose to improve bowel movements (Bell et al., 2009). In the present study, animals had free access to water and food to avoid behavioural stress that could influence gastrointestinal motility. Morphine was administered at a dose inducing slight yet significant constipation, so that co-treatment could modulate the effect. Regardless of the dose administered, CR4056 did not worsen morphine-induced constipation. And most importantly, there was no constipation when the low doses of CR4056 and morphine that have synergistic antihyperalgesic effects were combined.

The modulation of morphine-induced sedation by CR4056 was investigated because sedation is a sensitive indicator of impending respiratory depression related to opioid therapy (Pasero, 2009). Morphineinduced sedation in normal rats, as shown by a dose-dependent worsening of their locomotor activity and coordination. As with the other adverse effects analysed, co-administration of CR4056 with sedative doses of morphine did not worsen the opioid-induced sedative behaviour of rats. Rather, there was a trend for improvement, with a statistically significant change in sedation score at a dose of 6 $mg{\cdot}kg^{-1}$ CR4056. Once more, no differences were observed between rats treated with the low doses of CR4056 and morphine that synergize in analgesia and control animals.

Overall, the results of this study point towards a selective synergism between CR4056 and morphine for their analgesic activity, thus providing a strong rationale for use of CR4056 as an opioid-sparing drug in multimodal analgesia. CR4056 is the first I_2 receptor ligand to show analgesic activity in humans (Rovati et al., 2020), which supports clinical development as a non-opioid analgesic across a broad range of pain indications. Our present findings open a novel development path for CR4056 at low doses. Clinical trials should be rapidly set-up for use in combination with opioids, possibly resulting in decreased tolerance, opioid-induced adverse events, and abuse liabilities.

ACKNOWLEDGEMENTS

The authors wish to thank Mrs Francesca Colombo, Mrs Raffaella Miotto, Mr Dario Tremolada, Mr Luca Catapano, and Mrs Rosanna Cavagnoli for their skilful technical help, Dr Paolo Garofalo for his help in the analysis of data, and Mrs Laura Radaelli for secretarial assistance. Rottapharm Biotech funded this study.

AUTHOR CONTRIBUTIONS

E.S., F.F., M.L., C.M., C.S., E.C., M.B.F., and G.C. contributed in the process of data acquisition and in drafting the article. E.S., F.F., M.L., A.B., G.C., and L.C.R. contributed in the conception and design of the study, in the analysis and interpretation of data, and in the final approval of the version to be submitted. L.C.R. contributed also in obtaining of funding.

CONFLICT OF INTEREST

C.M. is a post-doctoral fellow with no conflicting interests. All the other authors are employees of Rottapharm Biotech.

DECLARATION OF TRANSPARENCY AND SCIENTIFIC RIGOUR

This Declaration acknowledges that this paper adheres to the principles for transparent reporting and scientific rigour of preclinical research as stated in the BJP guidelines for Design & Analysis, Immunoblotting and Immunochemistry, and Animal Experimentation and as recommended by funding agencies, publishers and other organisations engaged with supporting research.

ORCID

Emanuele Sala https://orcid.org/0000-0003-0472-1430
Marco Lanza https://orcid.org/0000-0001-7264-6386
Chiara Milia https://orcid.org/0000-0002-1835-8495
Chiara Sabatini https://orcid.org/0000-0002-8921-0279
Albino Bonazzi https://orcid.org/0000-0002-7857-5352
Gianfranco Caselli https://orcid.org/0000-0002-1075-7408
Lucio Claudio Rovati https://orcid.org/0000-0002-3425-1583

REFERENCES

Akbarali, H. I., Inkisar, A., & Dewey, W. L. (2014). Site and mechanism of morphine tolerance in the gastrointestinal tract. *Neurogastroenterology and Motility*, *26*, 1361–1367.

Alexander, S. P. H., Christopoulos, A., Davenport, A. P., Kelly, E., Mathie, A., Peters, J. A., … Yao, C. (2019). The concise guide to pharmacology 2019/20: G protein-coupled receptors. *British Journal of Pharmacology*, *176*, S21–S141. https://doi.org/10.1111/bph.14748

Alexander, S. P. H., Fabbro, D., Kelly, E., Mathie, A., Peters, J. A., Veale, E. L., … CGTP Collaborators. (2019). THE CONCISE GUIDE TO PHARMACOLOGY 2019/20: Enzymes. *British Journal of Pharmacology*, *176*, S297–S396. https://doi.org/10.1111/bph.14752

Al-Hasani, R., & Bruchas, M. R. (2011). Molecular mechanisms of opioid receptor-dependent signaling and behavior. *Anesthesiology*, *115*, 1363–1381. https://doi.org/10.1097/ALN.0b013e318238bba6

Bektas, N., Nemutlu, D., & Arslan, R. (2015). The imidazoline receptors and ligands in pain modulation. *Indian Journal of Pharmacology*, *47*, 472–478. https://doi.org/10.4103/0253-7613.165196

Bell, T. J., Panchal, S. J., Miaskowski, C., Bolge, S. C., Milanova, T., & Williamson, R. (2009). The prevalence, severity, and impact of opioid-induced bowel dysfunction: Results of a US and European patient survey (PROBE 1). *Pain Medicine*, *10*, 35–42. https://doi.org/10.1111/j.1526-4637.2008.00495.x

Benyamin, R., Trescot, A., Datta, S., Buenaventura, R., Adllaka, R., Sehgal, N., … Vallejo, R. (2008). Opioid complications and side effects. *Pain Physician*, *11*, S105–S120.

Bohn, L. M., Lefkowitz, R. J., & Caron, M. G. (2002). Differential mechanisms of morphine antinociceptive tolerance revealed in βarrestin-2 knock-out mice. *The Journal of Neuroscience*, *22*, 10494–10500.

Burford, N. T., Gerritz, S. W., Clark, M. J., Traynor, J. R., Wehrman, T. S., Alt, A., … O'Connell, J. (2013). Discovery of positive allosteric modulators and silent allosteric modulators of the μ-opioid receptor. *Proceedings of the National Academy of Sciences*, *110*, 10830–10835. https://doi.org/10.1073/pnas.1300393110

Cahill, C. M., Walwyn, W., Taylor, A. M. W., Pradhan, A. A. A., & Evans, C. J. (2016). Allostatic mechanisms of opioid tolerance beyond desensitization and downregulation. *Trends in*

14765381, 2020, 14, Downloaded from https://bpspubs.onlinelibrary.wiley.com/doi/10.1111/bph.15049 by University Studi Milano Bicocca, Wiley Online Library on [16/07/2024]. See the Terms and Conditions (https://onlinelibrary.wiley.com/terms-and-conditions) on Wiley Online Library for rules of use; OA articles are governed by the applicable Creative Commons License

Pharmacological Sciences, *37*, 963–976. https://doi.org/10.1016/j.tips.2016.08.002

Christie, M. J. (2008). Cellular neuroadaptations to chronic opioids: Tolerance, withdrawal and addiction. *British Journal of Pharmacology*, *154*, 384–396. https://doi.org/10.1038/bjp.2008.100

Chuck, T. L., McLaughlin, P. J., Arizzi-LaFrance, M. N., Salamone, J. D., & Correa, M. (2006). Comparison between multiple behavioral effects of peripheral ethanol administration in rats: Sedation, ataxia, and bradykinesia. *Life Sciences*, *79*, 154–161.

Comi, E., Lanza, M., Ferrari, F., Mauri, V., Caselli, G., & Rovati, L. C. (2017). Efficacy of CR4056, a first-in-class imidazoline-2 analgesic drug, in comparison with naproxen in two rat models of osteoarthritis. *Journal of Pain Research*, *10*, 1033–1043.

Curtis, M. J., Bond, R. A., Spina, D., Ahluwalia, A., Alexander, S. P. A., Giembycz, M. A., … McGrath, J. C. (2015). Experimental design and analysis and their reporting: New guidance for publication in *BJP*. *British Journal of Pharmacology*, *172*, 3461–3471. https://doi.org/10.1111/bph.12856

DeLeo, J. A., Tanga, F. Y., & Tawfik, V. L. (2004). Neuroimmune activation and neuroinflammation in chronic pain and opioid tolerance/-hyperalgesia. *The Neuroscientist*, *10*, 40–52.

Dieleman, J. L., Baral, R., Birger, M., Bui, A. L., Bulchis, A., Chapin, A., … Murray, C. J. L. (2016). US spending on personal health care and public health, 1996-2013. *JAMA*, *316*, 2627–2646. https://doi.org/10.1001/jama.2016.16885

Ferrari, F., Fiorentino, S., Mennuni, L., Garofalo, P., Letari, O., Mandelli, S., … Caselli, G. (2011). Analgesic efficacy of CR4056, a novel imidazoline-2 receptor ligand, in rat models of inflammatory and neuropathic pain. *Journal of Pain Research*, *4*, 111–125. https://doi.org/10.2147/JPR.S18353

González-Rodríguez, S., Poras, H., Menéndez, L., Lastra, A., Ouimet, T., Fournié-Zaluski, M. C., … Baamonde, A. (2017). Synergistic combinations of the dual enkephalinase inhibitor PL265 given orally with various analgesic compounds acting on different targets, in a murine model of cancer-induced bone pain. *Scandinavian Journal of Pain*, *14*, 25–38. https://doi.org/10.1016/j.sjpain.2016.09.011

Haleem, D. J., & Nawaz, S. (2017). Inhibition of reinforcing, hyperalgesic, and motor effects of morphine by buspirone in rats. *The Journal of Pain*, *18*, 19–28. https://doi.org/10.1016/j.jpain.2016.10.001

Harada, Y., Iizuka, S., Saegusa, Y., Mogami, S., Fujitsuka, N., & Hattori, T. (2017). Mashiningan improves opioid-induced constipation in rats by activating cystic fibrosis transmembrane conductance regulator chloride channel. *The Journal of Pharmacology and Experimental Therapeutics*, *362*, 78–84. https://doi.org/10.1124/jpet.117.240630

Harding, S. D., Sharman, J. L., Faccenda, E., Southan, C., Pawson, A. J., Ireland, S., … Davies, J. A. (2018). The IUPHAR/BPS guide to pharmacology in 2018: Updates and expansion to encompass the new guide to immunopharmacology. *Nucleic Acids Research*, *46*, D1091–D1106. https://doi.org/10.1093/nar/gkx1121

Horvath, R. J., Romero-Sandoval, E. A., & De Leo, J. A. (2010). Inhibition of microglial $P2X_4$ receptors attenuates morphine tolerance, Iba1, GFAP and μ opioid receptor protein expression while enhancing perivascular microglial ED2. *Pain*, *50*, 401–413.

Hucho, T. B., Dina, O. A., & Levine, J. D. (2005). Epac mediates a cAMP-to-PKC signaling ininflammatory pain: An isolectin B4(+) neuron-specific mechanism. *The Journal of Neuroscience*, *25*, 6119–6126.

Hudson, A. L., Gough, R., Tyacke, R., Lione, L., Lalies, M., Lewis, J., … Nutt, D. J. (1999). Novel selective compounds for the investigation of imidazoline receptors. *Annals of the new York Academy of Sciences*, *881*, 81–91. https://doi.org/10.1111/j.1749-6632.1999.tb09344.x

Hutchinson, M. R., Shavit, Y., Grace, P. M., Rice, K. C., Maier, S. F., & Watkins, L. R. (2011). Exploring the neuroimmunopharmacology of opioids: An integrative review of mechanisms of central immune signaling and their implications for opioid analgesia. *Pharmacological Reviews*, *63*, 772–810. https://doi.org/10.1124/pr.110.004135

Kabalak, A., Ekmekçioğlu, E., Ceylan, A., & Kahveci, K. (2013). The synergistic antinociceptive interactions of morphine and dexmedetomidine in rats with nerve-ligation injury. *Hippokratia*, *17*, 326–331.

Keller, B., & García-Sevilla, J. A. (2015). Immunodetection and subcellular distribution of imidazoline receptor proteins with three antibodies in mouse and human brains: Effects of treatments with I_1- and I_2-imidazoline drugs. *Journal of Psychopharmacology*, *29*, 996–1012.

Kilkenny, C., Browne, W., Cuthill, I. C., Emerson, M., & Altman, D. G. (2010). Animal research: Reporting in vivo experiments: The ARRIVE guidelines. *British Journal of Pharmacology*, *160*, 1577–1579. https://doi.org/10.1111/j.1476-5381.2010.00872.x

Kimura, A., Tyacke, R. J., Robinson, J. J., Husbands, S. M., Minchin, M. C., Nutt, D. J., & Hudson, A. L. (2009). Identification of an imidazoline binding protein: Creatine kinase and an imidazoline-2 binding site. *Brain Research*, *1279*, 21–28. https://doi.org/10.1016/j.brainres.2009.04.044

Kliewer, A., Schmiedel, F., Sianati, S., Bailey, A., Bateman, J. T., Levitt, E. S., … Schulz, S. (2019). Phosphorylation-deficient G-protein-biased μ-opioid receptors improve analgesia and diminish tolerance but worsen opioid side effects. *Nature Communications*, *10*, 367. https://doi.org/10.1038/s41467-018-08162-1

Lanza, M., Ferrari, F., Menghetti, I., Tremolada, D., & Caselli, G. (2014). Modulation of imidazoline I_2 binding sites by CR4056 relieves postoperative hyperalgesia in male and female rats. *British Journal of Pharmacology*, *171*, 3693–3701. https://doi.org/10.1111/bph.12728

Li, H. J., Li, C. J., Wei, X. N., Hu, J., Mu, D. L., & Wang, D. X. (2018). Dexmedetomidine in combination with morphine improves postoperative analgesia and sleep quality in elderly patients after open abdominal surgery: A pilot randomized control trial. *PLoS ONE*, *13*, e0202008. https://doi.org/10.1371/journal.pone.0202008

Li, J. X. (2017). Imidazoline I_2 receptors: An update. *Pharmacology & Therapeutics*, *178*, 48–56. https://doi.org/10.1016/j.pharmthera.2017.03.009

Liu, Y., Lu, G. Y., Chen, W. Q., Li, Y. F., Wu, N., & Li, J. (2018). Agmatine inhibits chronic morphine exposure-induced impairment of hippocampal neural progenitor proliferation in adult rats. *European Journal of Pharmacology*, *818*, 50–56.

Ma, X., Xu, T., Xu, H., & Jiang, W. (2015). Blockade and reversal of spinal morphine tolerance by P2X3 receptor antagonist. *Behavioural Pharmacology*, *26*, 260–267. https://doi.org/10.1097/FBP.0000000000000105

Manchikanti, L., Kaye, A. M., Knezevic, N. N., McAnally, H., Slavin, K., Trescot, A. M., … Hirsch, J. A. (2017). Responsible, safe, and effective prescription of opioids for chronic non-cancer pain: American Society of Interventional Pain Physicians (ASIPP) guidelines. *Pain Physician*, *20*, S3–S92.

McGrath, J. C., Drummond, G. B., McLachlan, E. M., Kilkenny, C., & Wainwright, C. L. (2010). Editorial: Guidelines for reporting experiments involving animals: The ARRIVE guidelines. *British Journal of Pharmacology*, *160*, 1573–1576. https://doi.org/10.1111/j.1476-5381.2010.00873.x

Mercadante, S. (2014). Efficacy and safety of dual opioid therapy. *Expert Opinion on Drug Safety*, *13*, 1433–1436. https://doi.org/10.1517/14740338.2014.966077

Meregalli, C., Ceresa, C., Canta, A., Carozzi, V. A., Chiorazzi, A., Sala, B., … Cavaletti, G. (2012). CR4056, a new analgesic I_2 ligand, is highly effective against bortezomib-induced painful neuropathy in rats. *Journal of Pain Research*, *5*, 151–167. https://doi.org/10.2147/JPR.S32122

Miranda, H. F., Prieto, J. C., Puig, M. M., & Pinardi, G. (2008). Isobolographic analysis of multimodal analgesia in an animal model of visceral acute pain. *Pharmacology, Biochemistry, and Behavior*, *88*, 481–486.

Mueller, D., Perdikaris, D., & Stewart, J. (2002). Persistence and drug-induced reinstatement of a morphine-induced conditioned place

14765381, 2020, 14, Downloaded from https://bpspubs.onlinelibrary.wiley.com/doi/10.1111/bph.15049 by University Studi Milano Bicocca, Wiley Online Library on [16/07/2024]. See the Terms and Conditions (https://onlinelibrary.wiley.com/terms-and-conditions) on Wiley Online Library for rules of use; OA articles are governed by the applicable Creative Commons License

preference. *Behavioural Brain Research*, *136*, 389–397. https://doi.org/10.1016/s0166-4328(02)00297-8

Nestler, E. J. (1997). Molecular mechanisms underlying opiate addiction: Implications for medications development. *Seminars in Neuroscience*, *9*, 84–93.

National Institute on Drug Abuse. Opioid overdose crisis. https://www.drugabuse.gov/drugs-abuse/opioids/opioid-overdose-crisis#five. Revised January 2019. Accessed March 2019

Ninković, J., & Roy, S. (2013). Role of the mu-opioid receptor in opioid modulation of immune function. *Amino Acids*, *45*, 9–24. https://doi.org/10.1007/s00726-011-1163-0

Pasero, C. (2009). Assessment of sedation during opioid administration for pain management. *J. Perianesthesia Nurs.*, *24*, 186–190.

Paxinos, G., and Watson, C. (1982). The rat brain in stereotaxic coordinates (Sidney).

Petruska, J. C., Cooper, B. Y., Johnson, R. D., & Gu, J. G. (2000). Distribution patterns of different P2x receptor phenotypes in acutely dissociated dorsal root ganglion neurons of adult rats. *Experimental Brain Research*, *134*, 126–132. https://doi.org/10.1007/s002210000414

Raffa, R. B. (2001). Pharmacology of oral combination analgesics: Rational therapy for pain. *Journal of Clinical Pharmacy and Therapeutics*, *26*, 257–264. https://doi.org/10.1046/j.1365-2710.2001.00355.x

Raghavendra, V., Tanga, F. Y., & DeLeo, J. A. (2004). Attenuation of morphine tolerance, withdrawal-induced hyperalgesia, and associated spinal inflammatory immune responses by propentofylline in rats. *Neuropsychopharmacology*, *29*, 327–334. https://doi.org/10.1038/sj.npp.1300315

Rovati, L. C., Brambilla, N., Blicharski, T., Connell, J., Vitalini, C., Bonazzi, A., … D'Amato, M. (2020). Efficacy and safety of the first-in-class imidazoline-2 receptor ligand CR4056 in pain from knee osteoarthritis and disease phenotypes: A randomized, double-blind, placebo-controlled phase 2 trial. *Osteoarthritis and Cartilage*, *28*, 22–30. https://doi.org/10.1016/j.joca.2019.09.002

Rudd, R. A., Seth, P., David, F., & Scholl, L. (2016). Increases in drug and opioid-involved overdose deaths—United States, 2010–2015. *MMWR. Morbidity and Mortality Weekly Report*, *65*, 1445–1452. https://doi.org/10.15585/mmwr.mm655051e1

Ruiz-Durántez, E., Torrecilla, M., Pineda, J., & Ugedo, L. (2003). Attenuation of acute and chronic effects of morphine by the imidazoline receptor ligand 2-(2-benzofuranyl)-2-imidazoline in rat locus coeruleus neurons. *British Journal of Pharmacology*, *138*, 494–500.

Sagar, D. R., Burston, J. J., Hathway, G. J., Woodhams, S. G., Pearson, R. G., Bennett, A. J., … Chapman, V. (2011). The contribution of spinal glial cells to chronic pain behaviour in the monosodium iodoacetate model of osteoarthritic pain. *Molecular Pain*, *7*, 88. https://doi.org/10.1186/1744-8069-7-88

Sastre, Ventayol, P., & García-Sevilla, J. A. (1996). Decreased density of I_2-imidazoline receptors in the postmortem brain of heroin addicts. *Neuroreport*, *7*, 509–512. https://doi.org/10.1097/00001756-199601310-00032

Shen, C. H., Tsai, R. Y., Shih, M. S., Lin, S. L., Tai, Y. H., Chien, C. C., & Wong, C. S. (2011). Etanercept restores the antinociceptive effect of morphine and suppresses spinal neuroinflammation in morphine-tolerant rats. *Anesthesia and Analgesia*, *112*, 454–459. https://doi.org/10.1213/ANE.0b013e3182025b15

Siemian, J. N., LaMacchia, Z. M., Spreuer, V., Tian, J., Ignatowski, T. A., Paez, P. M., … Li, J. X. (2018). The imidazoline I_2 receptor agonist 2-BFI attenuates hypersensitivity and spinal neuroinflammation in a rat model of neuropathic pain. *Biochemical Pharmacology*, *153*, 260–268. https://doi.org/10.1016/j.bcp.2018.01.032

Siemian, J. N., Obeng, S., Zhang, Y., Zhang, Y., & Li, J.-X. (2016). Antinociceptive Interactions between the imidazoline I_2 receptor agonist 2-BFI and opioids in rats: Role of efficacy at the μ-opioid receptor. *The Journal of Pharmacology and Experimental Therapeutics*, *357*, 509–519.

Siemian, J. N., Wang, K., Zhang, Y., & Li, J.-X. (2018). Mechanisms of imidazoline I_2 receptor agonist-induced antinociception in rats: Involvement of monoaminergic neurotransmission. *British Journal of Pharmacology*, *175*, 1519–1534.

Tallarida, R. J., Porreca, F., & Cowan, A. (1989). Statistical analysis of drug-drug and site-site interactions with isobolograms. *Life Sciences*, *45*, 947–961. https://doi.org/10.1016/0024-3205(89)90148-3

Thorn, D. A., Zhang, Y., & Li, J. X. (2016). Effects of the imidazoline I_2 receptor agonist 2-BFI on the development of tolerance to and behavioural/physical dependence on morphine in rats. *British Journal of Pharmacology*, *173*, 1363–1372. https://doi.org/10.1111/bph.13435

Trang, T., Al-Hasani, R., Salvemini, D., Salter, M. W., Gutstein, H., & Cahill, C. M. (2015). Pain and poppies: The good, the bad, and the ugly of opioid analgesics. *The Journal of Neuroscience*, *35*, 13879–13888. https://doi.org/10.1523/JNEUROSCI.2711-15.2015

van der Kam, E. L., De Vry, J., Schiene, K., & Tzschentke, T. M. (2008). Differential effects of morphine on the affective and the sensory component of carrageenan-induced nociception in the rat. *Pain*, *136*, 373–379. https://doi.org/10.1016/j.pain.2007.07.027

Varrassi, G., Fusco, M., Skaper, S. D., Battelli, D., Zis, P., Coaccioli, S., … Paladini, A. (2018). A pharmacological rationale to reduce the incidence of opioid induced tolerance and hyperalgesia: A review. *Pain and Therapy*, *7*, 59–75. https://doi.org/10.1007/s40122-018-0094-9

Vellani, V., & Giacomoni, C. (2017). Gabapentin inhibits protein kinase C epsilon translocation in cultured sensory neurons with additive effects when coapplied with paracetamol (acetaminophen). *The Scientific World Journal*, *2017*, 3595903.

Vellani, V., Sabatini, C., Milia, C., Caselli, G., Lanza, M., Letari, O., … Giacomoni, C. (2020). CR4056, a powerful analgesic imidazoline-2 receptor ligand, inhibits the inflammation-induced PKCε phosphorylation and membrane translocation in sensory neurons. *British Journal of Pharmacology*, *177*, 48–64. https://doi.org/10.1111/bph.14845

Volkow, N. D., & McLellan, A. T. (2016). Opioid abuse in chronic pain—Misconceptions and mitigation strategies. *The New England Journal of Medicine*, *374*, 1253–1263. https://doi.org/10.1056/NEJMra1507771

Williams, J. T., Christie, M. J., & Manzoni, O. (2001). Cellular and synaptic adaptations mediating opioid dependence. *Physiological Reviews*, *81*, 299–343.

SUPPORTING INFORMATION

Additional supporting information may be found online in the Supporting Information section at the end of this article.

How to cite this article: Sala E, Ferrari F, Lanza M, et al. Improved efficacy, tolerance, safety, and abuse liability profile of the combination of CR4056 and morphine over morphine alone in rodent models. *Br J Pharmacol*. 2020;177:3291–3308. https://doi.org/10.1111/bph.15049

14765381, 2020, 14, Downloaded from https://bpspubs.onlinelibrary.wiley.com/doi/10.1111/bph.15049 by University Studi Milano Bicocca, Wiley Online Library on [16/07/2024]. See the Terms and Conditions (https://onlinelibrary.wiley.com/terms-and-conditions) on Wiley Online Library for rules of use; OA articles are governed by the applicable Creative Commons License